

## Authors' response to reviewer #1

First of all, we would like to thank the reviewer for his careful reading and the very insightful and helpful comments. In the following, the reviewers' comments are in black, followed by our replies in blue. Modified and new text is in italic. The main changes in the revised manuscript are related to more thoroughly analysis of the orbit uncertainties related to time variable gravity field modeling and an analysis of the effects of the estimation of the DORIS system time bias on the radial orbit components of ascending and descending satellite passes.

### General Comments

\* The orbit error analysis is based on orbit differences, which exclude any error common to the orbits. This should be explicitly mentioned in the paper as well as the authors' assumptions in using orbit differences as an error estimate.

We agree with this comment. In addition to the already existing phrases we have included the following statements in the sections 'Introduction', 'Methods' and 'Summary and Conclusions'.

*Page 2, lines 61-62: Note, that our assessment necessarily excludes contributions from errors common to these three orbits.*

*Page 4, lines 94-95: The approach adopted for the estimation of the radial orbit errors implicates that errors common to all three orbits can not be detected. In particular, all three orbits rely on the ITRF2008 reference frame and basically the same set of tracking stations.*

*Page 7, lines 190-193: Since the radial orbit components map directly to the derived sea level heights, we consider the differences presented here to represent estimates of the orbit related sea level error. However, since the orbit error analysis is based on orbit differences, any error common to all three orbits will be lacking in our assessment.*

*Page 12, lines 354-355: We estimate the orbit errors from the radial orbit differences which implies that errors common to all orbits can not be detected.*

\* It seems the large and very similar REF-GRGS and REF-GSFC differences shown in Fig 5 could be better explained. Although similar in structure, the REF-Geoid plot features are so much smaller that one may exclude these gravity model differences as the primary cause of the REF-GRGS plot features. I suggest the authors include the GRGS-GSFC plot in the paper for which the orbits have much greater gravity model differences. I suspect much of the annual variability now shown is due to non-tidal station loading for the REF orbit. This contribution is not tested, but the GRGS-GSFC plot may help better identify the source of the annual variations.

We have included the GRGS-GSFC plot in the paper (Fig. 5) as suggested. We now interpret the results in more detail (page 9, lines 256-270) and come to the conclusion that modeling of the non-tidal station loading is a plausible source for part of the observed annual differences.

\* I also suggest running a spectral analysis on all the orbit differences to better identify all periodic signals; even if they are not evaluated they can be noted in the paper.

We have included plots of the power spectra of the global mean radial orbit differences for all orbit differences in the elctronical supplement (Fig. S2). We have added a short summary of the relevant periodic signals in Section 3.2.

Page 8, lines 229-233: *A spectral analysis of the global mean radial differences (Fig. S2) exhibits peaks at ~60 days for all but the GSFC and TBias orbit differences and at ~90 and ~170 days for the SLR and DORIS orbit differences. A weak annual component can be observed for the GRGS and Geoid orbit differences.*

\* The orbit trend differences are very small (Table 4), however Table 1 indicates substantial differences in the time variable gravity models. I suggest the authors describe/compare which gravity coefficient rates are used over the TOPEX period for all models, and which are defined by SLR.

We have provided in Table 1 more details on the time-variable Earth's gravity field modelling, namely, for which coefficients drift (linear) terms and annual and semi-annual variations are available. Additionally, we have added a new paragraph in Section 2.1 describing the Earth's time-variable gravity modeling for the three orbits (page 3, lines 83-93). To our experience differing drift terms of time variable gravity field models mainly induce dipole like patterns of regional trend differences (Table 5, Fig. 7). On the global mean these signals tend to cancel (Table 4).

\* This my main comment. The conclusion ends with a recommendation to try to better determine low-order gravity time-varying terms past the 5x5 field employed by the GSFC orbits using improved techniques with SLR/DORIS. The recommendation is not phrased clearly since the GSFC orbits show the lowest crossover residuals compared to the other test orbits which employ 50x50 and 80x80 time varying terms (Table 1). The problem for improving time variable gravity modeling over the TOPEX period should be an issue for all the orbits tested. The authors should mention this and clarify which time-varying terms are determined with SLR for the EIGEN-6S2 and EIGEN-6S4 fields over the TOPEX period and indicate the origin of the other terms. Furthermore the GSFC and Geoid orbit slightly improved performances over the REF orbit could suggest extrapolation of the higher order GRACE-defined seasonal terms to the TOPEX era may even be harmful. For example is the 5mm REF-Geoid annual signal (Fig 3) due to error in the REF orbit? The authors should clarify the conclusion in consideration of these remarks.

As mentioned in our response to the previous comment, we have specified in Table 1 and additionally described in Section 2.1 the details on modeling the Earth's time variable gravity. We further investigate and discuss the differences between the REF and the Geoid orbits at various places in more detail (page 6, lines 176-179; page7, lines 218-220; page 9, lines 269-270 and lines 285-288). We come to the conclusion that differences of the annual/semiannual terms of EIGEN-6S2 and EIGEN-6S4 for the pre-GRACE period are responsible for the enhanced performance of the Geoid with respect to the REF orbit. Differences of the regional interannual and decadal trends stem most probably from the yearly TVG terms derived from GRACE data starting from August 2002.

Additionally, we have replaced the last sentences of the Section "Summary and Conclusions" in order to clarify the conclusions (page 13, lines 409-419).

## Specific Comments

\* Any explanation why the DORIS residuals are slightly higher for the DORIS-only orbit? One would expect a decrease in the DORIS residuals compared to the DORIS+SLR orbit DORIS residuals.

We do not think, that the DORIS residuals of the DORIS-only orbit are necessarily smaller than those of DORIS+SLR orbit. In fact, the level of SLR and DORIS residuals for DORIS+SLR orbit is refined by the weighting of observation types (SLR and DORIS). In case, if SLR observations are given higher weight than DORIS observations, the SLR residuals of the SLR-only orbit should be smaller than those of the DORIS+SLR orbit and DORIS residuals of the DORIS-only orbit should be higher than those of the DORIS+SLR orbit. This is the case one observes in Table 2. This is, in fact, what is meant in the sentence "*This is related to the weighting of observations used (3 cm for SLR and 0.05 cm/s for DORIS) and to the number of observations used.*" on page 5, lines 139-140.

\* p7 l191 "The annual component of the global mean orbit differences is not included in Table 4, since it is not significant." Insignificant in amplitude, or is the formal error larger than the estimate?

Insignificant in amplitude, we have clarified this.

Page 8, line 232: *Since the annual amplitude is less than 1 mm only, it can be neglected and is not included in Table 4.*

\* p7 l212-216 non-tidal station loading for the REF orbits can also be included as a "plausible source" for annual orbit difference variations.

We agree with this comment. We have rephrased the paragraph.

Page 9, lines 265/266: *Another plausible source of the relatively strong signal for the GSFC and GRGS orbit cases are the differences in the annual corrections for station coordinates by geocenter motion corrections and non-tidal atmospheric loading.*

\* It is not clear what the REF-DORIS plot in Figure 5 is intended to show?

We have replaced this subplot by the corresponding plot for GRGS-GSFC. The whole paragraph is rephrased and the results are discussed in more detail.

\* It is interesting that the Figure 9 REF-DORIS plots show substantial trend differences for the ascending/descending passes. How is the considerable DORIS TOPEX network time bias treated for the various orbits? The SLR network should not have any significant time bias. It has been shown to be closely aligned with GPS time over the Jason-1 period (Zelensky et al. 2006, "DORIS time bias estimated using Jason-1")

In fact, the DORIS system time bias was estimated once per arc for the REF and GSFC orbits, and no bias correction was applied for the GRGS orbit. We have added this information in Table 1 and included a description and a plot of the DORIS time bias estimated with GFZ's orbits in Section 3.2 (Fig S1). Following your suggestions we have expanded our study. We have derived and analyzed an additional test orbit without adjustment of the DORIS time system. The corresponding analyses and results are described in Section 3.4.

\* p9 I264 “The most striking feature is that the ascending trends are opposite to the descending trends.” Say one orbit is always ahead of the other and will reach the North pole region (+Z) first, and the trend is positive. After reaching the North pole, the orbits will race South (-Z), and now will not the trend be negative?

We have rephrased the corresponding paragraph. Making use of the new test orbit we introduced, we observe in fact a strong relationship between the estimated DORIS time bias and the global mean radial orbit differences, anti-correlated for ascending and descending tracks. The regional pattern of the decadal trends is a coherent pattern over the Tropics and Subtropics. The same pattern shows up as leading pattern with about 60% explained variance from an EOF-analysis (see attached figure).

The DORIS system time bias is clearly related to along-track orbit position changes. A time bias of the altimeter measurement is known to induce (due to the latitude dependence of the altitude rate) radial errors which are anti-correlated for ascending and descending tracks (e.g. Scharro, R.: A Decade of ERS Orbits and Altimetry, PhD thesis, 2002, Fig. 5.1). However, the corresponding regional patterns would be different from the ones we observe, they should reveal a change of sign somewhere around the Tropics.

Even though our study shows, that uncertainties of the DORIS time bias are capable to induce ascending/descending discrepancies it does not fully explain the mechanism that transfers the along-track errors to radial orbit errors. However this question is beyond the scope of our paper and might be subject of a proper study. We have added a corresponding phrase at page 11, line 330: *This mechanism is not fully understood but a further analysis is beyond the scope of this paper.*

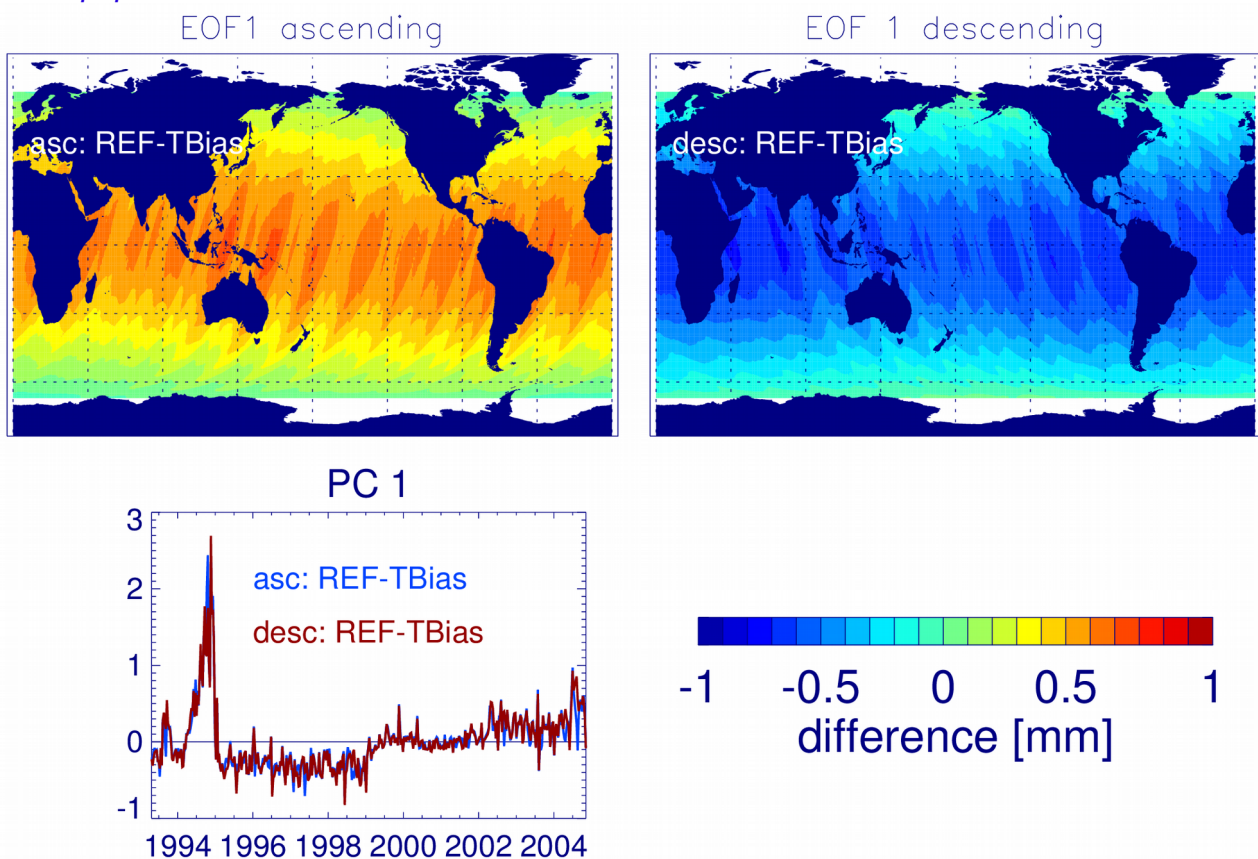


Figure: Leading pattern and time series derived from an EOF analysis of the *REF-TBias* orbit differences for ascending and descending passes.

# Orbit related sea level errors for TOPEX altimetry at seasonal to decadal time scales

Saskia Esselborn<sup>1</sup>, Sergei Rudenko<sup>1,2</sup>, Tilo Schöne<sup>1</sup>

<sup>1</sup>GFZ German Research Centre for Geosciences, [Department 1: Geodesy](#), Potsdam, 14473, Germany

5 <sup>2</sup>Deutsches Geodätisches Forschungsinstitut (DGFI-TUM), Technische Universität München, Munich, 80333, Germany  
(since August 2016, [until that – at GFZ](#))

*Correspondence to:* Saskia Esselborn (Saskia.Esselborn@gfz-potsdam.de)

**Abstract.** Interannual to decadal sea level trends are indicators of climate variability and change. A major source of global and regional sea level data is satellite radar altimetry, which relies on precise knowledge of the satellite's orbit. Here, we assess the error budget of the radial orbit component for the TOPEX/Poseidon mission for the period 1993 to 2004 from a set of different orbit solutions. Upper bound errors for seasonal, interannual (5 years), and decadal periods are estimated on global and regional scales based on radial orbit differences from three state-of-the-art orbit solutions provided by different research teams (GFZ, GSFC, and GRGS). The global mean sea level error related to the orbit is of the order of 7 mm (more than 10 % of the sea level variability) with negligible contributions on the annual and decadal time scale. In contrast, the orbit related error of the interannual trend is 0.1 mm/year (18 % of the corresponding sea level variability) and might hamper the estimation of an acceleration of the global mean sea level rise. For regional scales, the gridded orbit related error is up to 11 mm and for about half the ocean the orbit error accounts for at least 10 % of the observed sea level variability. The seasonal orbit error amounts to 10 % of the observed seasonal sea level signal in the Southern Ocean. At interannual and decadal time scales, the orbit related trend uncertainties reach regionally more than 1 mm/year. The interannual trend errors account for 10 % of the observed sea level signal in the Tropical Atlantic and the south-eastern Pacific. For decadal scales, the orbit related trend errors are prominent in a couple of regions including: South Atlantic, western North Atlantic, central Pacific, South Australian Basin, and Mediterranean Sea. Based on a set of test orbits calculated at GFZ, the sources of the observed orbit related errors are further investigated. Main contributors on all time scales are uncertainties in Earth's time variable gravity field models and on annual to interannual time scales discrepancies of the tracking station sub-networks, i.e., SLR and DORIS.

## 30 1 Introduction

Sea level is an important indicator of climate variability and change. Based on tide gauge data using different techniques, the global mean sea level rise for the last century is estimated to be 1.2-1.9 mm/year (Douglas, 1997; Church and White, 2011; Jevrejeva et al., 2008, 2014; Hay et al., 2015). Based on satellite altimetry data since 1993, the current rate of global mean sea level has been estimated to be more than 3 mm/year (Cazenave et al., 2014; Ablain et al., 2016; [Quartly et al., 2017](#)).

35 The main sources of the current rise are thermal expansion of the sea water and melting of glaciers and ice sheets. At interannual time scales, changes of terrestrial water storage imprint additionally on the global mean sea level (Llovel et al., 2011). Recent work ([Watson et al., 2015](#); [Fasullo et al., 2016](#)) has focussed on the detectability of accelerations in global mean sea level trends during the last decades ([Watson et al., 2015](#); [Fasullo et al., 2016](#)). Regionally, sea level rates during the last 24 years show higher variability, they range from -1 mm/year to more than 10 mm/year. They are mainly linked to regional changes in the oceans density field, which might be induced by internal ocean variability, atmosphere-ocean interaction, or influx of freshwater. Satellite altimeters are a unique source of global and regional sea level data and are available continuously since the beginning of the 1990s. Precise orbits of altimetry satellites are a precondition for global and regional mean sea level investigations (Rudenko et al., 2012; Rudenko et al., 2014) and errors related to precise orbit determination (POD) are demonstrably one of the major error sources for global and regional sea level products (Ablain et al., 2015). A detailed description of the main factors contributing to the radial orbit errors is given by Fu and Haines (2013). 45 The orbit errors have typically long  -wavelengths and may contain systematic contributions at seasonal to decadal timescales.

Couhert et al. (2015) investigated the main contributions to the radial orbit error budget for the Jason-1 and Jason-2 series based on Geophysical Data Records (GDR)-D at seasonal to decadal time scales for the second altimetry decade (2002- 50 2013). According to their analysis, the orbit related uncertainty of the global mean interannual and decadal trends is less than 0.1 mm/year. As main factors for regional errors they identified contributions from tracking data and from reference frame (up to 8 mm) at seasonal time scales, contributions from tracking data (up to 3 mm/year) and Earth's time variable gravity field (up to 2 mm/year) at interannual time scales, and contributions from tracking data (up to 2 mm/year) and Earth's time variable gravity field (up to 1.5 mm/year) at decadal time scales. A correspondent assessment for the first altimetry decade 55 (1992-2001) has still been ~~still~~ missing and is the rationale of this paper.

We assess the error budget of the radial orbit component for the TOPEX/Poseidon mission for the period 1993 to 2004 from a set of different orbit models. We have chosen TOPEX/Poseidon, since it is the reference altimetry mission used in the European Space Agency's (ESA) Climate Change Initiative (CCI) Sea Level project over this time span (Ablain et al., 2016). We assess the upper bound estimates of the radial orbit error budget at regional and global scales at seasonal, 60 interannual, and decadal time scales by the analysis of three state-of-the-art orbit solutions derived and provided by different research teams from the German Research Centre for Geosciences (GFZ), the Groupe de Recherche de Geodesie Spatiale (GRGS), and the Goddard Space Flight Centre (GSFC). Note, that our assessment necessarily excludes contributions from errors common to these three orbits. In our further analyses, we use test orbits calculated at GFZ to investigate the impact of

uncertainties of the tracking station sub-networks, of the reference frame, and of the Earth's time variable gravity field models on the radial orbit component, and hence the derived sea level.

A detailed description and assessment of the analysed orbits as well as specifications of the altimeter data processing are given in Sect. 2. Sect. 3 describes the methods implemented to assess the upper bound orbit errors for the different time scales and the corresponding results for global and regional scales. The main findings are summarized and discussed in Sect. 4.

## 70 | 2 Orbit and altimetry data

### 2.1 Description of the analysed orbit solutions

Our aim is to assess the range and the characteristics of radial orbit errors on regional and global scales. Therefore, the differences between three independent state-of-the-art orbit solutions available for the TOPEX/Poseidon mission are analysed. All orbit solutions are derived in the International Terrestrial Reference Frame (ITRF) 2008 reference frame (Altamimi et al., 2011) and use Satellite Laser Ranging (SLR) and Doppler Orbitography and Radiopositioning Integrated by Satellite (DORIS) tracking data, but are based on different software and on distinct models including different time variable gravity field models. The actual multi-mission GFZ orbit solution VER11 (Rudenko et al., 2017) is used as a reference in this paper and is called REF hereafter. The GSFC std1504 orbit (Lemoine et al., 2010; Beckley et al., 2015) has been chosen by the ESA CCI Sea Level Phase 2 project and differs in many aspects from the GFZ orbit, regarding software as well as the suite of implemented models including another Earth's gravity field model. As the third model, we have chosen the GRGS orbit solution (Soudarin et al., 2016), which is derived using models similar to those of the GFZ solution, but employing another software package. The main models used for GFZ REF, GRGS, and GSFC std1504 orbits are described in Table 1. The main differences in these three orbit solutions are related to the choice of the Earth's time variable gravity (TVG) field models, ocean tide model, modelling of non-tidal atmospheric and oceanic gravity, and the treatment of geocenter variations in station displacements. Proper modelling of the Earth's gravity field, in particular of its time-variable part, is crucial for the computation of precise orbits of altimetry satellites and has been shown to contribute to errors in regional sea level trends and seasonal signals (Rudenko et al., 2014; Esselborn et al., 2015). For the pre-GRACE period the TVG field is poorly constrained. The weekly TVG solutions used for the GSFC orbit were derived up to degree and order 5 from the analysis of SLR and DORIS observations to 20 geodetic satellites starting from 1993 (Lemoine et al., 2016). The TVG part used for the GFZ REF (GRGS) orbits consists of the combination of yearly coefficients, drift terms and annual and semi-annual variations for degree and order 1 to 80 (2 to 50) derived from GRACE data and SLR measurements to LAGEOS-1/2. The annual and semi-annual coefficients used for the GFZ REF orbit are fitted yearly starting from August 2002. For the pre-GRACE period before August 2002 (January 2003) only the degree 2 terms exhibit yearly values and drift terms, however, the annual and semi-annual variations, which were derived for the GRACE-period, are applied for degree and order 1-80 (2-50) (Rudenko et al., 2014, Förste et al., 2016).

The approach adopted for the estimation of the radial orbit errors implicates that errors common to all three orbits can not be detected. In particular, all three orbits rely on the ITRF2008 reference frame and basically the same set of tracking stations. To further estimate the orbit related radial orbit error budget due to the most significant factors, we have derived ~~five~~ test orbits based on the GFZ REF orbit. The errors related to inconsistencies of the tracking data networks are tested by using only one tracking network instead of two. Since the GRGS orbit was derived without estimation of the DORIS system time bias, we have studied the impact of this bias on the radial orbit differences with special focus on systematic differences between ascending and descending passes. The effect of errors in the realization of the terrestrial reference frame is tested by the implementation of the most recent ITRF2014 version.~~The tested factors include the consistency of the tracking data networks, The effects of uncertainties in Earth's TVG field models are tested by the implementation of the EIGEN-6S2 model which is the predecessor of the EIGEN-6S4 model the Earth's time variable gravity field model, and the realization of the terrestrial reference frame.~~ For each case, the same background models and estimated parameters were used as for the REF orbit, except for those that represent the changes for the specific test case. The ~~five~~ test orbits and the differences with respect to the GFZ REF orbit are:

- SLR orbit: derived by using SLR tracking observations only,
- DORIS orbit: computed by using DORIS tracking observations only,
- TBias orbit: calculated without estimation of the DORIS system time bias,
- ITRF14 orbit: calculated by using the information on station positions and velocities from ITRF2014 (Altamimi et al., 2016) instead of ITRF2008,
- Geoid orbit: obtained by using EIGEN-6S2 (Rudenko et al., 2014) Earth's gravity field model instead of EIGEN-6S4 model (Förste et al., 2016). Note that the Geoid orbit is based on the same gravity field model as the GRGS orbit.

## 2.2 TOPEX altimeter data

In order to assess the orbit accuracy at crossover points and to relate the estimated errors to the total variability of the sea level data, along-track TOPEX Sea Level v1.1 ECV data (Ablain et al., 2015<sup>6</sup>) released from the ESA CCI Sea Level project has been included in the analyses. The along-track data has been corrected for all instrumental and geophysical effects by the state-of-the-art models provided with the data. However, for some corrections updated models were applied. These include: the GSFC std1504 orbits, EOT11a ocean tides and loading tides (Savcenko and Bosch, 2012), solid earth tides following the IERS 2003 conventions, and updated GPD+ wet tropospheric corrections (Fernandes and Lazaro, 2016). The processing of the data, the crossover point and collinear analyses as well as the interpolation to a regular grid were performed using GFZ's Altimeter Database and Processing System (ADS) Central (Schöne et al., 2010).

### 2.3 Evaluation of the orbit solutions

In the following, the performance of the analysed orbits is evaluated. For the GFZ orbit solutions, the consistency with tracking data and at arc overlaps is assessed. Table 2 provides the main results of precise orbit determination of the GFZ reference and test orbits, namely, the average values of SLR and DORIS RMS fits, radial, cross-track, and along-track two-day arc overlaps, illustrating the internal orbit consistency in these directions, and the number of the arcs used to compute these values for the reference and ~~five~~ test orbits. Smaller values of arc overlaps and observation fits, when using the same observation types and weighting between them, indicate improved orbit quality. Reduced radial arc overlaps characterise reduced radial orbit error. SLR observations were used at all 494 orbital arcs of ~~five~~ GFZ orbits, except for the DORIS orbit for which no SLR observations were used at all. Since DORIS data are available for TOPEX/Poseidon only until October 31, 2004, these data were used at ~~433~~459 orbital arcs preceding this date, except for the SLR orbit for which no DORIS observations were used at all. All orbital arcs for GFZ orbits are manoeuvre-free. Thus, two-day arc overlaps were computed for 433 overlaps for the REF, TBias, ITRF14, and Geoid orbits. In case of the SLR and DORIS orbits, a few gaps in the observations caused radial arc overlap larger than 0.5 m. Those arc overlaps have been excluded from the statistics resulting in less arc overlaps shown for these orbits in Table 2.

Fig. ~~ures~~ 1 and 2 provide information on the quality of the reference and tests orbits. The ~~three~~four orbits derived using SLR and DORIS observations provide comparable levels of average SLR RMS fits (1.96 – 1.9~~7~~ cm, Fig. 1), ~~however, the largest value is obtained for the TBias orbit, when no DORIS system time bias is estimated~~. The smallest average SLR RMS fits (1.59 cm) are obtained with the orbit based on SLR observations only. This is related to the weighting of ~~the~~ observations used ~~-(3 cm for SLR observations and 0.05 cm/s for DORIS) observations and to the number of observations used~~. Among ~~four~~five orbits derived using DORIS observations, a slightly increased average value of DORIS RMS fits (0.04795 cm/s) is obtained for the DORIS orbit derived using only DORIS observations ~~followed by the TBias orbit (0.04785 cm/s)~~, while the ~~three~~other orbits derived using SLR and DORIS observations (REF, ITRF14, and Geoid) show comparable average values of DORIS RMS fits (0.04775 – 0.04778 cm/s). Fig. 2 shows two-day arc overlaps in the radial direction ~~for the GFZ REF and test orbits depending on the type of observations used for precise orbit determination: SLR-only, DORIS-only and SLR+DORIS data~~. The smallest average value of the radial overlaps (0.8~~3~~8 cm) is obtained using ~~DORIS-only observations~~the EIGEN-6S2 geopotential model. The radial arc overlaps of the TOPEX/Poseidon orbit derived using only SLR data are 1.95 times larger than those of the orbit derived using only DORIS data ~~(Fig. 2)~~. Using the reference frame ITRF2014 instead of ITRF2008 eliminates many outliers in the radial arc overlaps (Fig. 2) and therefore reduces the average value of the radial overlaps from 0.90 to 0.84 cm.

~~The DORIS system time bias is regularly estimated and applied during GFZ's POD process to adjust the DORIS time system to the SLR time system. Zelensky et al. (2006) have shown, that there is a strong linear relationship between along-track orbit position and the DORIS time bias. The comparison of the fits and overlap values of the REF and the TBias orbit (Table 2) show, that the estimation of the DORIS time bias improves the orbit quality. The temporal behaviour of the DORIS system time bias derived for TOPEX/Poseidon REF, ITRF14 and Geoid test orbits is in close agreement (Fig. S1) and~~

160 resembles the estimation given by Lemoine et al. (2016). For the GFZ VER11 (REF) orbit, it indicates variations between  
-22.4 microsecond ( $\mu\text{s}$ ) and  $+4.4 \mu\text{s}$  from 1992.73 to 1994.18, followed by a period of a linear trend of  $35.11 \mu\text{s}/\text{year}$  from  
1994.18 to 1995.00 that ends with a jump from  $-28.65 \mu\text{s}$  to  $+1.98 \mu\text{s}$  around 1995.00. Then the DORIS time bias shows two  
rather stable periods with a mean value of  $+3.70 \mu\text{s}$  with a standard deviation of  $1.77 \mu\text{s}$  from 1995.0 to 1999.0 and a mean  
values  $-1.32 \mu\text{s}$  with a standard deviation  $1.19 \mu\text{s}$  from 1999.0 to 2001.13, followed again by a period of a linear trend ( $-3.14$   
165  $\mu\text{s}/\text{year}$ ) from 2001.13 to 2004.83. The mean value of the DORIS system time bias is  $0.04 \pm 0.36 \mu\text{s}$  for the DORIS test  
orbit, and it is equal to zero (not shown in the figure) for the TBias orbit.

For all orbit solutions, a crossover point analysis for the period April 1993 to ~~Nov~~September 2004 has been performed based  
on the altimeter data described in Sect. 2.2above. Differences between the values of ascending and descending ~~passetraeks~~  
at crossover points are caused by oceanic variability and errors related to the measurements, the orbit, and the applied  
170 corrections. Since in our study errors related to the measurements and the applied corrections and oceanic variability are  
always identical, here, smaller absolute mean differences and decreased RMS values at crossover points are indicative for  
increased orbit quality. The median of the time series of global mean height differences and RMS values at the crossover  
points are provided in Table 3. The smallest ascending/descending differences ( $-1.6 \text{ mm}$ ) and as well the lowest RMS values  
( $49.5 \text{ mm}$ ) at the crossover points are reached by the GSFC orbit solution. The mean global ascending/descending  
175 differences are  $-3.1 \text{ mm}$  for the GFZ REF and  $-2.9 \text{ mm}$  for the GRGS orbit solutions. However, while the RMS value of the  
GFZ REF solution ( $49.8 \text{ mm}$ ) is comparable to the one of the GSFC, the GRGS orbit solution shows degraded performance  
( $51.3 \text{ mm RMS}$ ). Keeping the DORIS time bias fixed to zero deteriorates the mean differences between ascending and  
descending passes to  $-3.6 \text{ mm}$  but does not change the RMS value. The median of the global mean ascending/descending  
differences is  $-2.7 \text{ mm}$  for the SLR and  $-4.7 \text{ mm}$  for the DORIS orbits. Both orbit solutions show degraded performance  
180 ( $51.1/50.7 \text{ mm RMS}$ ) with respect to the REF solution. This shows that using SLR and DORIS observations together  
improves the orbit quality considerably, even though the DORIS observations seem to aggravate the mean differences  
between ascending and descending tracks. Using ITRF2014 instead of ITRF2008 does not change the crossover point  
statistics. The Geoid orbit solution exhibits clearly improved ascending/descending differences ( $-2.1 \text{ mm}$ ) and as well a  
slight reduction of the RMS values. A further analysis of the temporal evolution of the ascending/descending differences  
185 reveals, that these improvements take place in the pre-GRACE period before August 2002.

### 3 Estimation of the orbit related sea level error

Sea level is varying on typical temporal and spatial scales, that are often connected to the driving processes. At the same  
time, orbit errors are not randomly distributed but exhibit also typical temporal and spatial pattern. Here, we apply statistical  
methods in order to assess upper bound errors related to the orbit solutions for global and regional sea level at seasonal to  
190 decadal time scales.

### 3.1 Methods

In order to estimate upper limits for orbit related errors in sea level height, the differences between the radial components of the GFZ REF orbit and the two independent orbit solutions (GSFC and GRGS) have been analysed. To assess the effect of uncertainties in the reference system, in the realisation of the tracking station networks, and in Earth's time variable gravity  
195 on the radial error budget, we have evaluated the differences of the radial orbit components between the GFZ's REF and ITRF14, SLR, DORIS, and Geoid test orbits. Since the radial orbit components map directly to the derived sea level heights, we consider the differences presented here to represent estimates of the orbit related sea level error. However, since the orbit error analysis is based on orbit differences, any error common to all three orbits will be lacking in our assessment.

The differences of the radial orbit components at the time of the altimetry measurement (1 Hz, ~6.7 km on ground) are  
200 calculated and interpolated to a global  $1^\circ \times 1^\circ$  grid for every cycle (9.92 days). In general, we merge both, ascending and descending, passtracks in our calculations. In addition, we analyse ascending and descending passtracks for some orbit combinations separately.

For the regional analyses, starting from the gridded radial orbit differences, the RMS values relative to the local temporal mean are calculated for each grid point over the entire time series. Decadal trends, annual and semi-annual signals, and the  
205 corresponding formal errors are estimated by a least-square fit. As a measure for errors at interannual time scales, we calculate the RMS of the five-years running trend series of the radial orbit differences at each grid point. Regional upper bound errors are guessed from the corresponding maximum RMS values over the ocean at the  $1^\circ \times 1^\circ$  grid.

For the global analyses, the gridded radial orbit differences are averaged (with area weighting) over the ocean ( $\pm 67^\circ$  latitude). Starting from these global mean height differences, global mean RMS, decadal trend, annual cycle, and the RMS of  
210 the five-years running trends series are derived, based on the same methods as used for the regional analyses. Global mean RMS values per cycle are calculated as the square root of the spatial mean of the radial orbit differences at each grid point over the ocean for the respective cycle.

In order to relate the estimated errors to the total variability of the sea level data, TOPEX altimeter data has been included as well. The data and the processing is described in Sect. 2.2. From the gridded sea level anomalies, seasonal, interannual and  
215 decadal trends were derived using the methods described above.

### 3.2. Global mean errors

In the following, we investigate the orbit related global sea level error, differentiating between the total error and its annual, interannual, and decadal components. The TBias orbit differences are not included in these analyses but will be further investigated for the study of changes between ascending and descending passes (Sect. 3.4). The time series of the global  
220 mean RMS of gridded radial orbit differences per cycle are shown in Fig. 3 for all orbit solutions relative to GFZ's REF orbit. The largest differences occur between the REF and the GRGS orbits, the smallest changes occur for the ITRF14 test orbit. Most orbit differences are dominated by sub-seasonal variability, only the Geoid and ITRF14 orbit differences are governed by seasonal and decadal periods. For the Geoid, GSFC, and GRGS orbit differences relative to the REF orbits, the

RMS series exhibit a seasonal cycle, which is an indication for seasonal orbit differences on regional scales. The RMS of the REF minus Geoid orbit difference is decreased after August 2002 indicating that the main differences between the two orbits originate from the pre-GRACE period. In contrast, the differences between the REF and the ITRF14 orbits are slightly increasing from 2000 onwards. The orbit errors derived from the analysis of the global mean orbit difference series over the oceans are summarized in Table 4 for all orbit models together with the corresponding absolute sea level values. The global mean RMS of the radial orbit differences between the REF and GRGS (GSFC) orbits amount to 7.0 (5.4) mm, which corresponds to more than 10 % of the global mean sea level variability of 52.5 mm. The restriction to one tracking station sub-network leads to large changes of the orbit, for the DORIS (SLR) orbit solution the RMS values of the radial differences with respect to the REF orbit amount to 5.1 mm (4.2 mm), which is almost of the size of the estimated upper bound orbit errors. This highlights the importance of manifold, precise, and consistent tracking data for accurate global mean sea level estimates. The substitution of the Earth's gravity field model (EIGEN-6S4 by EIGEN-6S2) and the ITRF realization (ITRF2008 by ITRF2014) accounts for 2.0 mm and 1.1 mm, respectively, of the mean orbit errors. A spectral analysis of the global mean radial differences (Fig. S2) exhibits peaks at ~60 days for all but the GSFC and TBias orbit differences and at ~90 and ~170 days for the SLR and DORIS orbit differences. A weak annual component can be observed for the GRGS and Geoid orbit differences. Since the annual amplitude is less than 1 mm only, it can be neglected and~~The annual component of the global mean orbit differences~~ is not included in Table 4, ~~since it is not significant.~~ The time series of the five-years running trends of the global mean radial orbit differences over the ocean are shown in Fig. 4 for the various orbit combinations. All curves range between  $\pm 0.2$  mm/year and show at least one zero-crossing and imply, which interannual changes of the estimated decadal sea level trends is consistent with small changes of the decadal trends. The corresponding curve of the five-years running trends for the global mean sea level (not shown) are much larger, they range between 4 mm/year at the beginning of the time series and 2 mm/year at the end (not shown). Before 1998~~At the beginning of the time series;~~ the GSFC and GRGS solutions are close to each other and both suggest ~~smaller interannual trends than the GFZ solution before 1998~~ larger sea level trends for this period than the GFZ solution. After that, trends derived from GFZ and GSFC orbits show good agreement, while the GRGS solution ~~exhibits smaller trends results in somewhat higher trends till 2001~~ which would result in smaller sea level trends for this period when using the GRGS orbit. Maximum interannual trend variability of 0.1 mm/year occurs between the REF and GRGS orbits (Table 4) which amounts to almost 20 % of the corresponding value derived for the global mean sea level curve (0.55 mm/year). Hence, the use of the GFZ instead of the GRGS orbit should result in a slightly stronger acceleration of the mean sea level curve during the TOPEX period. Since the exclusive use of DORIS tracking station leads to interannual trend variability of 0.1 mm/year, inconsistencies of the tracking stations sub-networks ~~are capable might~~ to explain large portions of the observed global mean interannual variability. The errors of the interannual trend variability are for all orbit combinations higher than for the decadal trends. The global mean decadal trends (calculated over the full mission time) are mostly significant but can be further neglected, since they are two orders of magnitude smaller than the observed sea level signal over this period ( $\sim 3$  mm/year).

### 3.3 Regional errors

The maximum regional errors derived from the analysis of the gridded orbit difference series over the oceans are summarized in Table 5. ~~The TBias orbit differences are not included in these analyses but will be further investigated for the study of changes between ascending and descending passes (Sect. 3.4).~~ Regionally, the maximum radial orbit differences on the  $1^\circ \times 1^\circ$  grid between the REF and GRGS (GSFC) orbits amount to 10.7 (7.4) mm. The exclusive use of only one tracking station sub-network leads to distinct changes with RMS values of 9.3 mm (7.2) mm for the DORIS (SLR) sub-network. This suggests that ~~for the weighting factors applied with GFZ's REF orbit~~ especially inhomogeneity in the SLR station sub-network has the potential to produce ~~consider~~notable regional orbit errors.

Annual difference signals with respect to the REF orbit are most prominent for the GSFC and GRGS solutions, while they are negligible for the SLR, DORIS, and ITRF14 orbits. The corresponding patterns of ~~the~~ annual amplitudes for the differences of REF versus GSFC, GRGS, ~~DORIS~~, and Geoid orbits ~~and of GRGS versus GSFC orbits~~ are shown in Fig. 5. ~~Plausible sources of the relatively strong signal for the GSFC and GRGS orbit cases are the differences in the used Earth's time variable gravity field models, the use of AOD1B products instead of ECMWF data for the reference orbit, and differences in the annual corrections for station coordinates.~~ The observed patterns for the GSFC and GRGS orbit differences consist of ~~the a dipole with centers in the southeastern Indian Ocean and the Caribbean. Since the two centres are phase shifted by half a year, the effect on the global mean differences is marginal. superposition of two dipoles oriented north/south and east/west. The east/west oriented dipole pattern~~The pattern coincides with the patterns already shown to be related to the use of AOD1B products (Rudenko et al., 2016) and different Earth's time variable gravity fields for TOPEX/Poseidon POD (Esselborn et al., 2016). ~~However, the annual differences between the REF and Geoid orbits can only explain part of the observed differences between the REF and GRGS orbits. In addition, the annual differences between GRGS and GSFC orbits are quite small and show no distinct pattern. Another plausible source of the relatively strong signal for the GSFC and GRGS orbit cases are the differences in the annual corrections for station coordinates by geocenter motion corrections and non-tidal atmospheric loading. The thorough reflection of the relevant models used for the POD of these three orbits suggests, that the observed differences originate in part from the non-tidal atmospheric loading effect on the stations which was applied for the GFZ but not the GRGS and GSFC orbits. There is evidence, that the annual signal from the EIGEN-6S2 gravity field model is closer to the solution applied for the GSFC orbits than to EIGEN-6S4 – at least in the pre-GRACE period. The north/south oriented dipole pattern corresponds to variations in the z-component of the reference system which is consistent with annual geocentre motions variations described for the Jason-2 mission by Melachroinos et al. (2013). The same pattern is also observed for the annual signal of the DORIS minus REF orbit differences.~~

The patterns of the interannual variability of the regional trends are shown in Fig. 6 for all orbit differences. The trend errors reach up to 1.2 (0.9) mm/year for the GSFC (GRGS) orbit differences (Table 5). The patterns of the trend variability from the GSFC and GRGS differences show coinciding maxima in the regions around South America and Australia. The differences for the Geoid orbit show similar features even though the absolute trend variability is smaller (up to 0.4 mm/year). For the SLR and DORIS orbit differences, the patterns of interannual variability (Fig. 6) are patchy and oriented

along individual tracks. For the ITRF14 solution, the trend variability is slightly increased at high latitudes (up to 0.2 mm/year). The patterns of the interannual trend variability derived from the GFZ test orbits suggest, that differences in the TVG modelling and contributions from the tracking systems are the most plausible sources of the observed regional differences of trend variability between REF, GSFC, and GRGS orbits.

295 The strongest regional changes in the decadal trend (Fig. 7 and Table 5) are observed for the differences between the REF and GSFC orbits (up to 1.0 mm/year). For the GSFC orbit, high absolute decadal trend differences tend to coincide with maximum seasonal differences, but not with maximum interannual variability. The differences between the REF and GRGS orbit trends reach 0.7 mm/year at maximum—and show similar patterns as the differences between REF and Geoid orbit trends (up to 0.4 mm/year). Here, and the patterns of maximum annual amplitudes, interannual and decadal trend differences  
300 coincide. The differences between the REF and Geoid orbit trends resemble these patterns, however, the trend values are smaller (up to 0.4 mm/year) and can explain only about half of the observed decadal trend differences. The source of decadal trends between EIGEN-6S2 and EIGEN-6S4 during the TOPEX period are presumably differences in the modelling of the TVG after August 2002, since before drift terms are only applied to degree 2 terms. The degree 2 terms, in turn, are defined by SLR data and show close agreement between the two TVG models for the pre-GRACE period. The ITRF14 orbit  
305 differences drift locally by a rate of up to 0.2 mm/year with positive values in the southern hemisphere and negative values in the northern hemisphere, indicating a drift in the z-component between the reference system realisations. The observed values are in good agreement with the combined change of scale and rate of the z-component of the transformation between ITRF2008 and ITRF2014 (Altamimi et al., 2016). The regional decadal trends for the SLR and DORIS orbit differences are patchy and rather related to particular tracks without consistent long-wavelength behaviour. Higher trends of up to 0.4  
310 mm/year emerge for the DORIS orbit. The patterns of the decadal trend differences derived from the GFZ test orbits suggest, that differences in the TVG modelling are the most plausible source of the observed regional trend differences between REF, GSFC, and GRGS orbits.

~~Our analysis exhibits large scale patterns of the orbit related error. How do these relate to the patterns of sea level variability? Fig. 8 shows the sea level variability, seasonal signal, interannual and decadal trends derived from ESA CCI TOPEX altimeter data for those regions where the orbit error amounts to at least 10 % of the corresponding sea level value. This allows us to define regions where the orbit related error should be considered when analysing the sea level data. For about half the ocean the orbit error accounts for at least 10 % of the observed sea level variability. This is especially the case for calm oceanic regions, whereas for energetic regions like the Circumpolar Current, Tropical Pacific, and the western boundary currents of the northern hemisphere the dynamic ocean signal is much larger than the orbit error. For the seasonal signal, mainly the Southern Ocean is affected. The influence of the orbit error on the interannual trend variability is important in the Tropical and Subtropical Atlantic and the south-eastern Pacific. The estimation of the decadal trend may be hampered by orbit errors in the following regions: central Pacific, South Atlantic, western North Atlantic, south-eastern Indian Ocean, but also in several marginal seas including the Mediterranean, Red Sea, Yellow Sea and Sea of Japan.~~

315  
320

### 3.4 Differences between ascending and descending passetracks

325 The crossover point analysis (Table 3) reveals considerable global mean differences between ascending and descending  
passes for most orbits. Fu and Haines (2013) have shown, that orbit errors might induce diverging drifts for sea level derived  
from ascending and descending passes. orbit errors might reveal diverging drifts for ascending and descending tracks (e.g.,  
Fu and Haines, 2013). In the following, we study whether there are systematic changes to the results obtained so far when  
ascending and descending passes are investigated separately. From our crossover point analysis (Table 3), we have chosen  
330 the three orbit solutions revealing the largest RMS values, i.e., GRGS, DORIS, and SLR. For these orbits solutions,  
wTherefore, e performed the for a subset of orbit solutions the same analyses were performed as before, but separately but  
for data sets derived from ascending and descending trackpasses only. Since the DORIS orbit reveals the most pronounced  
median ascending/descending differences we have chosen to study the REF minus DORIS and the REF minus TBias orbit  
differences further. During the POD of the GRGS orbit, the DORIS system time bias is not estimated, therefore, we include  
335 the GRGS orbit in the analysis as well. However, in contrast to the previous analysis, we study the difference Geoid minus  
GRGS instead of REF minus GRGS in order to exclude the effects of different time variable gravity fields from the  
resultsanalysis.

The global mean radial orbit differences for ascending and descending passes are for all three cases in the range of  $\pm 12$  mm  
(Fig. S3). The ascending and descending radial orbit differences are significantly anti-correlated. The correlation coefficient  
340 is almost -1 for the REF minus TBias case, almost -0.9 for the Geoid minus GRGS case, and still -0.5 for the REF minus  
DORIS case. The correlation is further increased for periods of more than one year. The REF minus TBias global mean time  
series resembles the DORIS system time bias applied for the REF orbit (Fig. S1). The global mean radial differences for the  
Geoid minus GRGS case reveal similar features as well. All three orbit differences exhibit diverging global mean radial  
differences for ascending and descending tracks after the year 2000.

345 The interannual trend variability and decadal trends derived from the analysis of the global mean radial orbit difference  
series over the oceans are summarized in Table 6 for the merged, ascending, and descending trackpasses. If the ascending  
and descending trackpasses are analysed separately, the interannual trend variability is increased by at least about 5 five  
times for the corresponding orbit differences. Ascending passes exhibit higher variability than the descending. There are notable  
discrepancies of the global mean decadal trends (up to 0.3 mm/year) between ascending and descending tracks for the REF  
350 minus SLR, REF minus DORIS, and Geoid minus GRGS differences. The most striking feature is that the ascending trends  
are opposite to the descending trends. The differences for the global mean decadal trends between ascending and descending  
passes are a multiple of the values for the merged data and reach up to 0.6 mm/year, where both data sets are drifting in  
opposite directions.

The regional patterns of the decadal trend differences for ascending and descending trackpasses are shown in Fig. 89. The  
355 SLR and DORIS orbit differences reveal a striking spread between the decadal trends of the ascending and descending  
trackpasses. The trends are opposite for ascending and descending trackpasses for most areas of the global ocean and reach  
regionally absolute values of up to 0.8 mm/year. Trends for the REF minus TBiasSLR orbit differences are very similar but

360 smaller ~~than and opposite to~~ the *REF minus DORIS* orbit ones. The corresponding analysis for the *Geoid minus GRGS* orbit differences, ~~which share the same Earth's time variable gravity field model~~, shows again very similar features as for the DORIS differences. ~~To further investigate the relation between ascending and descending tracks, we calculated the principal components of the gridded orbit difference time series. The pattern of the leading component for all analysed ascending and descending difference grids are large scale and correspond to variations of Earth's pole flattening. The corresponding time series of the ascending and descending series are highly anti-correlated for frequencies lower than 1 year (-0.91 for REF minus SLR, -0.95 for REF minus DORIS, and -0.87 for Geoid minus GRGS).~~ This indicates that discrepancies in the reference systems of the tracking stations (distribution of tracking stations, observation sampling, etc.) might give rise to long-wavelength orbit errors being anti-correlated for ascending and descending ~~trackpasses~~. Relevant contributions are originating from uncertainties of the timing of the DORIS measurements. Increasing time biases are related to increasing along-track position errors and seem to be transferred to radial orbit errors. This mechanism is not fully understood but a further analysis is beyond the scope of this paper. The uncertainties are especially pronounced in tropical and subtropical regions. On regional scales, the interannual and decadal trend errors derived from ascending/descending ~~trackpasses~~ separately can be many times higher reach twice than the values derived from the merged data. Even though such effects tend to cancel, whenever both components are merged, they might still introduce considerable errors in regional studies, that are based on along-track data, e.g. at calibration sites.

### **3.5 Regional orbit errors and sea level variability**

375 Our analysis exhibits large scale patterns of the orbit related error. Errors for interannual to decadal sea level trends of more than 1 mm/year might hamper the interpretation of the observed sea level variability from altimetry, at least apart from the large oceanic currents. In order to define regions where the orbit related error should be considered when analysing sea level data from TOPEX, we have determined areas with orbit errors of at least 10 % of the corresponding sea level value. Fig. 9 shows the sea level variability, seasonal signal, interannual and decadal trends derived from ESA CCI TOPEX altimeter data for those regions where the orbit error amounts to at least 10. % of the corresponding sea level value. Taking into account the total orbit related error, about half the ocean is affected. This includes especially calm oceanic regions, whereas for energetic regions like the Circumpolar Current, Tropical Pacific, and the western boundary currents of the northern hemisphere the dynamic ocean signal is much larger than the orbit error. For the seasonal signal, mainly the Southern Ocean is concerned. Critical regions for the estimation of the interannual variability are the Tropical and Subtropical Atlantic and the south-eastern Pacific. For decadal scales, the orbit related trend errors are prominent in a couple of regions including: South Atlantic, western North Atlantic, central Pacific, and south-eastern Indian Ocean, but also several marginal seas including the Mediterranean, Red Sea, Yellow Sea and Sea of Japan.

## 4 Summary and Conclusions

We have investigated the radial orbit error budget associated with [three](#) state-of-the-art orbit solutions [from GFZ, GSFC and GRGS](#) over the first altimetry decade (1993-2004). It is crucial to know the accuracy of these early altimeter data in order to judge the reliability of long-term sea level trends and of estimations of the acceleration of global mean sea level rise. For this purpose, we have chosen the TOPEX/Poseidon mission, since it is the reference altimetry mission used in ESA's CCI Sea Level project over this time span. [We estimate the orbit errors from the radial orbit differences which implies that errors common to all orbits can not be detected. A set of five test orbit solutions derived at GFZ is used to estimate the contributions of the most significant factors to the error budget.](#)~~In our analyses, w~~ We have focused on the impact of uncertainties of the tracking station sub-networks (SLR and DORIS), of the reference frame, and of the Earth's time variable gravity field models on the radial orbit component, and hence the derived sea level. The estimates of the upper bound radial orbit errors at seasonal, interannual (5 years), and decadal time scales are given in Table 4 for the global mean sea level and in Table 5 for the regional sea level.

According to our study, the global mean RMS radial orbit errors for the TOPEX period are of the order of 7 mm, which corresponds to more than 10 % of the global mean sea level variability (52 mm). The global mean annual (seasonal) component of the radial error [is below 1 mm and](#) can be neglected. The orbit related errors of the decadal trends are less than 0.05 mm/year and should not induce any significant artificial global mean sea level trends. However, on time scales of five years the trend variability may reach up to 0.1 mm/year, which amounts to almost 20 % of the corresponding sea level variability (0.55 mm/year), and could potentially hamper the detection of [sea level acceleration](#)~~interannual sea level signals~~ from the altimeter data. The major contributions to this error [\(0.04 – 0.10 mm/year\)](#) are, most probably, discrepancies of the station sub-networks (DORIS or SLR) used. The contributions of Earth's time variable gravity field model and the ITRF realisation (ITRF2008 [versus](#) ITRF2014)-~~to the global mean error~~ are of only minor importance [\(0.02 mm/year\)](#). [These values are in line with the mean upper bound orbit errors given by Couhert et al. \(2015\) derived for Jason-1 and Jason-2 orbits for the second altimetry decade \(2002-2012\).](#)

For regional scales, the maximum RMS of the gridded radial orbit error is more than 10 mm ~~derived from the two state-of-the-art orbit solutions GFZ REF (VER11) and GRGS~~. However, this error includes a large fraction of sub-seasonal variability which is not subject of this study. The regional upper bound error of the seasonal signal is 6 mm, of the interannual trend variability 1.2 mm/year, and of the decadal trend 1 mm/year. [Errors for interannual to decadal sea level trends of more than 1 mm/year might hamper the interpretation of the observed sea level variability from altimetry. For about half of the ocean outside the energetic regions \(e.g. Circumpolar Current, Tropical Pacific, Gulf Stream and Kuroshio System\) the orbit related errors reach at least 10% of the observed sea level variability. For the seasonal signal, mainly the Southern Ocean is concerned. Critical regions for the estimation of the interannual variability are the Tropical and Subtropical Atlantic and the south-eastern Pacific. For decadal scales, the orbit related trend errors are prominent in a couple of regions including: South Atlantic, western North Atlantic, central Pacific, and south-eastern Indian Ocean, but also several marginal seas including the Mediterranean, Red Sea, Yellow Sea and Sea of Japan.](#)

When using ascending and descending passes separately, the interannual and decadal trend errors can reach multiples of the values derived from the merged data. This is the case for global mean values as well as for regional values. The corresponding large scale pattern is coherent for low and medium latitudes and is strongly anti-correlated for ascending and descending passes. Even though such effects tend to cancel, whenever both components are merged, they might still introduce considerable errors in regional studies, that are based on along-track data, e.g. at calibration sites.

~~as estimated from the difference between the GFZ REF and the GSFC std1504 orbit solutions.~~

Orbit errors related to discrepancies between the tracking station sub-networks (distribution of tracking stations, observation sampling, etc.) are studied based on GFZ's SLR, DORIS, and TBias orbit solutions. Using both SLR and DORIS observations for TOPEX POD together reduces (improves) the RMS of the altimetry single-satellite crossover differences considerably (2-3%), though the DORIS observations seem to aggravate the mean differences between ascending and descending passes. The proper estimation of the DORIS system time bias has proven to be a critical factor for the minimization of this effect. The most significant changes are observed for the DORIS orbit solution suggesting that uncertainties of the SLR station sub-network should have the most prominent effects on the orbit accuracy – at least for GFZ's orbit solutions. This fact is, most probably, related to the weighting factors applied to the observations within the GFZ orbit determination process. Using the latest reference frame ITRF2014 instead of the predecessor ITRF2008 slightly improves the accuracy of the TOPEX/Poseidon orbit solution. The contribution of the uncertainties in the ITRF realisation to the regional upper bound error is only marginal. Errors induced by uncertainties of the Earth's time variable gravity field model are studied on the base of GFZ's Geoid orbit solution. The orbit evaluations show that the Geoid orbit performs slightly better than the REF orbit in the pre-GRACE period due to differences in the time-invariant annual and semiannual variations applied to the TVG field models. Uncertainties of the gravity field model give rise to orbit errors at all analysed periods, and the corresponding patterns show close agreement with the ones derived from the GFZ and the external orbit differences. We estimate regional upper bound errors of ~3 mm for the seasonal signal and of 0.4 mm/year for the interannual trend variability and the decadal trend. This accounts for about 60 % of the seasonal, about 30 % of the interannual, and about 40 % of the decadal orbit error which are related to differences between EIGEN-6S2 and EIGEN-6S uncertainties of the time variable gravity field models. However, these values might be still underrated due to the similarity of the two time variable gravity field models used for GFZ's REF und Geoid orbit solutions.4.

The regional upper bound radial orbit errors obtained from our study are by factor 2 to 5 smaller than the ones reported by Couhert et al. (2015) for the period 2002 to 2012. This might partly reflect recent improvements of the stability of reference frames which result in smaller changes from ITRF2008 to ITRF2014 than previously from ITRF2005 to ITRF2008. However, the accuracy of the Earth's time variable gravity model and the tracking observations for the 1990's should be inferior to more recent periods. The error related to the uncertainties of the tracking station sub-networks might be underrated in our study since all analysed orbits rely on basically the same set of tracking observations. The effect of uncertainties of the time variable gravity (TVG) field might be underestimated as well since EIGEN-6S4 and EIGEN-6S2 both model the TVG field in the pre-GRACE period by time-invariant annual and semi-annual variations derived from

GRACE plus annual values and drift terms for degree two terms derived from SLR measurements. In contrast, the TVG field used for the GSFC orbit determination is weekly changing. Using SLR measurements to geodetic cannon-ball satellites (Sośnica et al., 2015, Bloßfeld et al., 2016) and in combination with DORIS measurements to altimetry and remote sensing satellites (Lemoine et al., 2016) allows to determine Earth's time variable gravity for the period 1993-2003, i.e. before GRACE, more precisely than just using SLR measurements to LAGEOS-1/2. Combined use of SLR and DORIS measurements to numerous geodetic satellites, especially for 1990-2003, with the GRACE measurements should further improve Earth's time variable gravity field models and hence further enhance orbit solutions for the ERS and the TOPEX/Poseidon altimetry missions. Orbit errors related to discrepancies between the tracking station sub-networks (distribution of tracking stations, observation sampling, etc.) are studied based on GFZ's SLR and DORIS orbit solutions. Using both SLR and DORIS observations for TOPEX POD together reduces (improves) the RMS of the altimetry single-satellite crossover differences considerably, though the DORIS observations seem to aggravate the mean differences between ascending and descending tracks. Hence, the restriction to only one tracking station sub-network has considerable regional effects on the orbit solutions. The most significant changes are observed for the DORIS orbit solution suggesting that uncertainties of the SLR station sub-network should have the most prominent effects on the orbit accuracy—at least for GFZ's orbit solutions. This fact is, most probably, related to the weighting factors applied to the observations within the GFZ orbit determination process. The seasonal errors related to the exclusive use of the DORIS tracking station sub-network are maximum at high latitudes (up to 2 mm) and are conform to uncertainties in the z-coordinate of the orbit's reference system. For interannual and decadal time scales, the errors related to the exclusive use of the DORIS tracking station sub-network are patchy and rather oriented along single satellite tracks with most pronounced errors at interannual time scales (up to 0.6 mm/year). However, when using ascending or descending tracks separately, the interannual and decadal trend errors can reach twice the values derived from the merged data. The corresponding large scale patterns correspond to variations of Earth's pole flattening and are anti-correlated for ascending and descending tracks on time scales of more than one year. Even though such effects tend to cancel, whenever both components are merged, they might still introduce considerable errors in regional studies, that are based on along-track data, e.g. at calibration sites. Using ITRF2014 instead of ITRF2008 slightly improves the accuracy of the orbit solution as shown by the orbit evaluation. The contribution of the uncertainties in the ITRF realisation (ITRF2014 versus ITRF2008) to the regional upper bound error is only marginal, with maximum seasonal signals of 0.4 mm and interannual to decadal signals of 0.2 mm/year.

Our analysis exhibits large scale patterns of the orbit related error. Errors for interannual to decadal sea level trends of more than 1 mm/year might hamper the interpretation of the observed sea level variability from altimetry, at least apart from the large oceanic currents. In order to define regions where the orbit related error should be considered when analysing sea level data from TOPEX, we have determined areas with orbit errors of at least 10 % of the corresponding sea level value. Taking into account the total orbit related error, about half the ocean is affected. For the seasonal signal, mainly the Southern Ocean is concerned. Critical regions for the estimation of the interannual variability are the Tropical and Subtropical Atlantic and the south-eastern Pacific. For decadal scales, the orbit related trend errors are prominent in a couple of regions including:

490 South Atlantic, western North Atlantic, central Pacific, and south-eastern Indian Ocean, but also several marginal seas including the Mediterranean, Red Sea, Yellow Sea and Sea of Japan.

Our estimation of the global mean upper bound orbit errors for the first altimetry decade is in line with the numbers given by Couhert et al. (2015) derived for Jason-1 and Jason-2 orbits for the second altimetry decade (2002-2012). However, the regional upper bound radial orbit errors obtained from our study are somewhat smaller than the ones reported by Couhert et al. (2015) for the second decade. This might partly reflect recent improvements of the stability of reference frames which result in smaller changes from the ITRF2008 to ITRF2014 reference frame. However, the accuracy of the Earth's time variable gravity model and the tracking observations for the 1990's is inferior to more recent periods. Potentially, the error related to the uncertainties of the tracking station sub-networks is underrated in our study since all analysed orbits rely on basically the same set of tracking observations. For the POD of the GSFC std1504 orbits, Earth's time variable gravity field has been modelled up to degree and order 5 based on DORIS and SLR data. In the future, POD for the TOPEX period might benefit from further improved Earth's time variable gravity field models making use of DORIS (Cerri et al., 2013) and SLR data (Sośnica et al., 2015).

## 505 **Acknowledgements**

We are grateful for the insightful comments of the reviewer Dr. Nikita Zelensky which helped to improve the manuscript substantially. We thank Goddard Space Flight Centre and Groupe de Recherche de Geodesie Spatiale for the provision of GSFC\_std1504 and GRGS orbit solutions, ESA CCI for along-track TOPEX Sea Level v1.1 ECV data, and Joana Fenandes for the provision of updated wet troposphere corrections (GPD+). This research was partly supported by the European Space Agency (ESA) within the Climate Change Initiative Sea Level (SLCCI) Phase II project and by the Deutsche Forschungsgemeinschaft (DFG) through grant (CoRSEA) as part of the Special Priority Program (SPP)-1889 "Regional Sea Level Change and Society" (SeaLevel) and within the projects "Consistent dynamic satellite reference frames and terrestrial geodetic datum parameters" and "Interactions of low-orbiting satellites with the surrounding ionosphere and thermosphere (INSIGHT)" and by the International Office of the BMBF under the grant 01DO17017 "Sea Level Change and its Hazardous Potential in the East China Sea and Adjacent Waters" (SEAHAP).

## References

- 520 Ablain, M., Cazenave, A., Valladeau, G. and Guinehut, S.: A new assessment of the error budget of global mean sea level rate estimated by satellite altimetry over 1993–2008, *Ocean Sci.*, 5(2), 193–201, doi:10.5194/os-5-193-2009, 2009.
- Ablain, M., Cazenave, A., Larnicol, G., Balmaseda, M., Cipollini, P., Faugère, Y., Fernandes, M. J., Henry, O., Johannessen, J. A., Knudsen, P., Andersen, O., Legeais, J., Meyssignac, B., Picot, N., Roca, M., Rudenko, S., Scharffenberg, M. G., Stammer, D., Timms, G. and Benveniste, J.: Improved sea level record over the satellite altimetry era (1993–2010) from
- 525 the Climate Change Initiative project, *Ocean Sci.*, 11(1), 67–82, doi:10.5194/os-11-67-2015, 2015.
- Ablain, M., Legeais, J. F., Prandi, P., Marcos, M., Fenoglio-Marc, L., Dieng, H. B., Benveniste, J. and Cazenave, A.: Satellite Altimetry-Based Sea Level at Global and Regional Scales, *Surv. Geophys.*, 1–25, doi:10.1007/s10712-016-9389-8, 2016.
- Altamimi, Z., Collilieux, X. and Métivier, L.: ITRF2008: an improved solution of the international terrestrial reference
- 530 frame, *J. Geod.*, 85(8), 457–473, doi:10.1007/s00190-011-0444-4, 2011.
- Altamimi, Z., Rebischung, P., Métivier, L. and Collilieux, X.: ITRF2014: A new release of the International Terrestrial Reference Frame modeling nonlinear station motions, *J. Geophys. Res. Solid Earth*, 121(8), 2016JB013098, doi:10.1002/2016JB013098, 2016.
- Beckley, B., Ray, R., Holmes, S., Zelensky, N., Lemoine, F., Yang, X., Brown, S., Desai, S., Mitchum, G. and Hausman, J.:
- 535 Integrated Multi-Mission Ocean Altimeter Data for Climate Research TOPEX/Poseidon, Jason-1 and OSTM/Jason-2 User's Handbook Version 3.0, pp. 61, California Institute of Technology, [ftp://podaac.jpl.nasa.gov/allData/merged\\_alt/L2/TP\\_J1\\_OSTM/docs/v121415.version3.0\\_multi\\_alt\\_handbook.pdf](ftp://podaac.jpl.nasa.gov/allData/merged_alt/L2/TP_J1_OSTM/docs/v121415.version3.0_multi_alt_handbook.pdf) (Accessed May 2017), 2015.
- [Bloßfeld, M., Stefka, V., Müller, H., and Gerstl M.: Satellite laser ranging - a tool to realize GGOS? In: Rizos C., Willis P. \(Eds.\) IAG 150 Years, IAG Symposia 143, 540-547, doi:10.1007/1345\\_2015\\_202, 2016](#)
- 540 Boehm, J. and Schuh, H.: Vienna mapping functions in VLBI analyses, *Geophys. Res. Lett.*, 31(1), L01603, doi:10.1029/2003GL018984, 2004.
- Carrère, L., Lyard, F., Cancet, M., Roblou, L. and Guillot, A.: FES 2012: a new tidal model taking advantage of nearly 20 years of altimetry measurements, OSTST meeting, September 22-29, Venice-Lido, Italy, [online] Available from:
- 545 [http://www.avisio.altimetry.fr/fileadmin/documents/OSTST/2012/oral/01\\_thursday\\_27/03\\_tides/04\\_TID\\_Carrere2.pdf](http://www.avisio.altimetry.fr/fileadmin/documents/OSTST/2012/oral/01_thursday_27/03_tides/04_TID_Carrere2.pdf) (Accessed May 2017), 2012.
- Cazenave, A., Dieng, H.-B., Meyssignac, B., von Schuckmann, K., Decharme, B. and Berthier, E.: The rate of sea-level rise, *Nature Clim. Change*, 4(5), 358–361, doi:10.1038/nclimate2159, 2014.
- Cerri, L. and Ferrage, P.: DORIS satellites models implemented in POE processing, CNES, Paris, France, Tech. Rep. SALP-NTBORD-OP-16137-CN, Rev. 10, [online] Available from: [ftp://ftp.ids-](ftp://ftp.ids-doris.org/pub/ids/satellites/DORISSatelliteModels.pdf)
- 550 [doris.org/pub/ids/satellites/DORISSatelliteModels.pdf](ftp://ftp.ids-doris.org/pub/ids/satellites/DORISSatelliteModels.pdf) (Accessed May 2017), 2016.
- [Cerri, L., Lemoine, J. M., Mercier, F., Zelensky, N. P. and Lemoine, F. G.: DORIS-based point mascons for the long term stability of precise orbit solutions, Adv. Space Res., 52\(3\), 466–476, doi:10.1016/j.asr.2013.03.023, 2013.](#)
- Church, J. A. and White, N. J.: Sea-Level Rise from the Late 19th to the Early 21st Century, *Surv. Geophys.*, 32(4–5), 585–
- 555 602, doi:10.1007/s10712-011-9119-1, 2011.

- Couhert, A., Cerri, L., Legeais, J.-F., Ablain, M., Zelensky, N. P., Haines, B. J., Lemoine, F. G., Bertiger, W. I., Desai, S. D. and Otten, M.: Towards the 1 mm/y stability of the radial orbit error at regional scales, *Adv. Space Res.*, 55(1), 2–23, doi:10.1016/j.asr.2014.06.041, 2015.
- 560 Dobslaw, H., Flechtner, F., Bergmann-Wolf, I., Dahle, C., Dill, R., Esselborn, S., Sasgen, I. and Thomas, M.: Simulating high-frequency atmosphere-ocean mass variability for dealiasing of satellite gravity observations: AOD1B RL05, *J. Geophys. Res. Oceans*, 118(7), 3704–3711, doi:10.1002/jgrc.20271, 2013.
- Douglas, B. C.: Global Sea Rise: A Redetermination, *Surv. Geophys.*, 18(2–3), 279–292, doi:10.1023/A:1006544227856, 1997.
- 565 Esselborn, S., Schöne, T. and Rudenko, S.: Impact of Time Variable Gravity on Annual Sea Level Variability from Altimetry, in *IAG 150 Years*, pp. 55–62, Springer, Cham., doi:10.1007/1345\_2015\_103, 2015.
- Fasullo, J. T., Nerem, R. S. and Hamlington, B.: Is the detection of accelerated sea level rise imminent?, *Scientific Reports*, 6, 31245, doi:10.1038/srep31245, 2016.
- Fernandes, M. J. and Lázaro, C.: GPD+ Wet Tropospheric Corrections for CryoSat-2 and GFO Altimetry Missions, *Remote Sensing*, 8(10), 851, doi:10.3390/rs8100851, 2016.
- 570 Förste, C., Bruinsma, S., Abrikosov, O., Rudenko, S., Lemoine, J.-M., Marty, J.-C., Neumayer, K. H. and Biancale, R.: EIGEN-6S4 A time-variable satellite-only gravity field model to d/o 300 based on LAGEOS, GRACE and GOCE data from the collaboration of GFZ Potsdam and GRGS Toulouse, [online] Available from: <https://doi.org/10.5880/icgem.2016.008> (Accessed May 2017), 2016.
- 575 Fu, L.-L. and Haines, B. J.: The challenges in long-term altimetry calibration for addressing the problem of global sea level change, *Adv. Space Res.*, 51(8), 1284–1300, doi:10.1016/j.asr.2012.06.005, 2013.
- Goiginger, H., Hoeck, E., Rieser, D., Mayer-Guerr, T., Maier, A., Krauss, S., Pail, R., Fecher, T., Gruber, T. and Brockmann, J.: The combined satellite-only global gravity field model GOCO02S, *Geophysical Research Abstracts*, 13, EGU2011-10571, [online] Available from: <http://www.goco.eu/data/egu2011-10571-goco02s.pdf> (Accessed May 2017), 2011.
- 580 Hedin, A. E.: MSIS-86 Thermospheric Model, *J. Geophys. Res.: Space Physics*, 92(A5), 4649–4662, doi:10.1029/JA092iA05p04649, 1987.
- Hay, C. C., Morrow, E., Kopp, R. E. and Mitrovica, J. X.: Probabilistic reanalysis of twentieth-century sea-level rise, *Nature*, 517(7535), 481–484, doi:10.1038/nature14093, 2015.
- 585 IERS Conventions (2003), McCarthy, D.D. and Petit, G. (Eds.): Bundesamt für Kartographie und Geodäsie, Frankfurt am Main. [online] Available from: <http://www.iers.org/TN32> (Accessed May 2017), 2004.
- IERS Conventions (2010), Petit, G. and Luzum, B. (Eds.): Bundesamt für Kartographie und Geodäsie, Frankfurt am Main. [online] Available from: <https://www.iers.org/TN36> (Accessed May 2017), 2010.
- Jevrejeva, S., Moore, J. C., Grinsted, A. and Woodworth, P. L.: Recent global sea level acceleration started over 200 years ago?, *Geophys. Res. Lett.*, 35(8), L08715, doi:10.1029/2008GL033611, 2008.
- 590 Jevrejeva, S., Moore, J. C., Grinsted, A., Matthews, A. P. and Spada, G.: Trends and acceleration in global and regional sea levels since 1807, *Global and Planetary Change*, 113, 11–22, doi:10.1016/j.gloplacha.2013.12.004, 2014.
- ~~Knocke, P. and Ries, J.: Earth Radiation Pressure Effects on Satellites, Technical Memorandum, Center for Space Research, the University of Texas at Austin, Austin, Texas, 1987.~~

- Knocke, P., Ries, J. and Tapley, B.: Earth radiation pressure effects on satellites, in AIAA Paper 88-4292, pp. 577–587, 595 Austin, TX, United States, 1988.
- Lemoine, F. G., Zelensky, N. P., Chinn, D. S., Pavlis, D. E., Rowlands, D. D., Beckley, B. D., Luthcke, S. B., Willis, P., Ziebart, M., Sibthorpe, A., Boy, J. P. and Luceri, V.: Towards development of a consistent orbit series for TOPEX, Jason-1, and Jason-2, *Adv. Space Res.*, 46(12), 1513–1540, doi:10.1016/j.asr.2010.05.007, 2010.
- Lemoine, F. G., Chinn, D. S., Zelensky, N. P., Beall, J. W. and Le Bail, K.: The development of the GSFC DORIS 600 contribution to ITRF2014, *Adv. Space Res.*, 58(12), 2520–2542, doi:10.1016/j.asr.2015.12.043, 2016.
- Llovel, W., Becker, M., Cazenave, A., Jevrejeva, S., Alkama, R., Decharme, B., Douville, H., Ablain, M. and Beckley, B.: Terrestrial waters and sea level variations on interannual time scale, *Glob. Planet. Change*, 75(1–2), 76–82, doi: 10.1016/j.gloplacha.2010.10.008, 2011.
- Lyard, F., Lefevre, F., Letellier, T. and Francis, O.: Modelling the global ocean tides: modern insights from FES2004, *Ocean Dyn.*, 56(5–6), 394–415, doi:10.1007/s10236-006-0086-x, 2006.
- Masters, D., Nerem, R. S., Choe, C., Leuliette, E., Beckley, B., White, N. and Ablain, M.: Comparison of Global Mean Sea Level Time Series from TOPEX/Poseidon, Jason-1, and Jason-2, *Marine Geodesy*, 35(sup1), 20–41, doi:10.1080/01490419.2012.717862, 2012.
- ~~Melachroinos, S. A., Lemoine, F. G., Zelensky, N. P., Rowlands, D. D., Luthcke, S. B. and Bordyugov, O.: The effect of geocenter motion on Jason-2 orbits and the mean sea level, *Adv. Space Res.*, 51(8), 1323–1334, doi:10.1016/j.asr.2012.06.004, 2013.~~ 610
- Mendes, V. B. and Pavlis, E. C.: High-accuracy zenith delay prediction at optical wavelengths, *Geophys. Res. Lett.*, 31(14), L14602, doi:10.1029/2004GL020308, 2004.
- Pavlis, E. C., SLRF2008: The ILRS reference frame for SLR POD contributed to ITRF2008, presented at the Ocean Surf. 615 Topogr. Sci. Team Meeting, Seattle, WA, USA, Jun. 2009. [online] Available from: [http://www.avisioceanobs.com/fileadmin/documents/OSTST/2009/poster/Pavlis\\_2.pdf](http://www.avisioceanobs.com/fileadmin/documents/OSTST/2009/poster/Pavlis_2.pdf) (Accessed May 2017), 2009.
- Quartly, G. D., Legeais, J.-F., Ablain, M., Zawadzki, L., Fernandes, M. J., Rudenko, S., Carrère, L., García, P. N., Cipollini, P., Andersen, O. B., Poisson, J.-C., Mbajon Njiche, S., Cazenave, A., Benveniste, J.: A new phase in the production of quality-controlled sea level data, *Earth Syst. Sci. Data*, 9(2), 557-572, doi:10.5194/essd-9-557-2017, 2017.
- Ray, R. D.: Precise comparisons of bottom-pressure and altimetric ocean tides, *J. Geophys. Res. Oceans*, 118(9), 4570–4584, 620 doi:10.1002/jgrc.20336, 2013.
- Ries, J.: Annual geocenter motion from space geodesy and models, abstract G12A-08, AGU Fall Meeting, San Francisco, 9-13 December 2013, [online] Available from: <http://ids-doris.org/images/documents/report/publications/AGU2013-AnnualGeocenterMotion-Ries.pdf> (Accessed May 2017), 2013.
- Rudenko, S., Otten, M., Visser, P., Scharroo, R., Schöne, T. and Esselborn, S.: New improved orbit solutions for the ERS-1 625 and ERS-2 satellites, *Adv. Space Res.*, 49(8), 1229–1244, doi:10.1016/j.asr.2012.01.021, 2012.
- Rudenko, S., Dettmering, D., Esselborn, S., Schöne, T., Förste, C., Lemoine, J.-M., Ablain, M., Alexandre, D. and Neumayer, K.-H.: Influence of time variable geopotential models on precise orbits of altimetry satellites, global and regional mean sea level trends, *Adv. Space Res.*, 54(1), 92–118, doi:10.1016/j.asr.2014.03.010, 2014.

- 630 Rudenko, S., Dettmering, D., Esselborn, S., Fagiolini, E. and Schöne, T.: Impact of Atmospheric and Oceanic De-aliasing Level-1B (AOD1B) products on precise orbits of altimetry satellites and altimetry results, *Geophys. J. Int.*, 204(3), 1695–1702, doi:10.1093/gji/ggv545, 2016.
- Rudenko, S., Neumayer, K.-H., Dettmering, D., Esselborn, S., Schöne, T. and Raimondo, J.-C.: Improvements in precise orbits of altimetry satellites and their impact on mean sea level monitoring, *IEEE Trans. Geosci. Remote Sens.*, 55(6), 635 3382–3395, doi:10.1109/TGRS.2017.2670061, 2017.
- Savcenko, R. and Bosch, W.: EOT11a-empirical ocean tide model from multi-mission satellite altimetry, DGFI Report 89, [online] Available from: [http://epic.awi.de/36001/1/DGFI\\_Report\\_89.pdf](http://epic.awi.de/36001/1/DGFI_Report_89.pdf) (Accessed May 2017), 2012.
- Schöne, T., Esselborn, S., Rudenko, S. and Raimondo, J.-C.: Radar Altimetry Derived Sea Level Anomalies – The Benefit of New Orbits and Harmonization, in *System Earth via Geodetic-Geophysical Space Techniques*, edited by F. M. Flechtner, 640 T. Gruber, A. Güntner, M. Manda, M. Rothacher, T. Schöne, and J. Wickert, pp. 317–324, Springer Berlin Heidelberg, Berlin, Heidelberg. [online] Available from: <http://edoc.gfz-potsdam.de/gfz/16014> (Accessed May 2017), 2010.
- Sośnica, K., Jäggi, A., Meyer, U., Thaller, D., Beutler, G., Arnold, D. and Dach, R.: Time variable Earth’s gravity field from SLR satellites, *J. Geod.*, 89, 945–960~~146~~, doi:10.1007/s00190-015-0825-1, 2015.
- Soudarin, L., Capdeville, H. and Lemoine, J.-M.: Activity of the CNES/CLS Analysis Center for the IDS contribution to 645 ITRF2014, *Adv. Space Res.*, 58(12), 2543–2560, doi:10.1016/j.asr.2016.08.006, 2016.
- Watson, C. S., White, N. J., Church, J. A., King, M. A., Burgette, R. J. and Legresy, B.: Unabated global mean sea-level rise over the satellite altimeter era, *Nature Clim. Change*, 5(6), 565–568, doi:10.1038/nclimate2635, 2015.
- Willis, P., Zelensky, N. P., Ries, J., Soudarin, L., Cerri, L., Moreaux, G., Lemoine, F. G., Otten, M., Argus, D. F. and Heflin, 650 M. B.: DPOD2008: A DORIS-Oriented Terrestrial Reference Frame for Precise Orbit Determination, in *IAG 150 Years*, pp. 175–181, Springer, Cham., doi: 10.1007/1345\_2015\_125, 2015.
- [Zelensky, N.P., Berthias, J.-P., Lemoine, F.G.: DORIS time bias estimated using Jason-1, TOPEX/Poseidon and ENVISAT orbits, J Geod., 80, 497–506. doi:10.1007/s00190-006-0075-3, 2006.](#)

655

660

665

**Table 1. The main models used for calculation of GFZ VER11, GSFC std1504 and GRGS orbits**

Parameter	GFZ REF (VER11) orbit	GSFC std1504 orbit	GRGS orbit
Terrestrial reference frame	ITRF2008 (Altamimi et al., 2011), SLRF2008 (Pavlis 2009), DPOD2008 (Willis et al., 2016)	ITRF2008, SLRF2008, DPOD2008	ITRF2008, SLRF2008, DPOD2008
Polar motion and UT1	IERS EOP 08 C04 (IAU2000A) series with IERS diurnal and semi-diurnal variations	IERS Bulletin A daily (consistent with ITRF2008), diurnal and semi-diurnal variations	IERS EOP 08 C04
Precession and nutation model	IERS Conventions (2010)	IAU2000	IERS 2010 using non-rotating origin
Station displacements due to annual geocenter variations	None	Ries (2013)	None
Non-tidal atmospheric loading effect on stations	Based on ECMWF ERA-Interim data	None	None
Ocean loading effect on stations	FES2004 (Lyard et al., 2006)	GOT4.10 (Ray, 2013)	FES2012 (Carrère et al., 2012)
Static Earth's gravity field model	EIGEN-6S4 (Förste et al., 2016) degree/order 81-90	GOCO2S ( $> d/o \leq 5$ ) (Goiginger et al., 2011)	EIGEN-6S2 (Rudenko et al., 2014)
Time-variable Earth's gravity field model	EIGEN-6S4 <a href="#">degree 2: yearly value and drift term, time-invariant (semi-)annual variations for d/o 1-80 from 15.8.2002: yearly values, drift terms and (semi-)annual variations for d/o 1-80.-</a>	Updated harmonic piecewise fit weekly solutions (Lemoine et al., 2016) up to d/o 5	EIGEN-6S2 <a href="#">degree 2: yearly value and drift term, time in-variant (semi-)annual variations for d/o 2-50 from 1.1.2003: yearly values and drift terms for d/o 2-50</a>
Solid Earth tide	IERS Conventions (2010)	IERS Conventions (2003)	IERS Conventions (2010)
Ocean tide model	EOT11a (Savchenko and	GOT4.10 up to d/o 50	FES2012 up to d/o 50

	Bosch, 2012) up to d/o 80		
Non-tidal atmospheric and oceanic gravity	<del>GFZ AOD1B RL05 up to d/o 100 (Dobslaw et al, 2013), including ECMWF 6-hourly fields and GFZ AOD1B RL05 (Dobslaw et al, 2013) up to d/o 100</del> OMCT	ECMWF 6-hourly fields up to d/o 50	3-hourly ERA-interim and TUGO R12 up to d/o 50
Atmospheric density model	MSIS-86 (Hedin, 1987)	MSIS-86	DTM 94, with best available solar activity data
Earth radiation and albedo	Knocke <del>et al. (1988)</del> and <del>Ries (1987)</del>	Knocke et al. (1988)	Albedo and IR pressure values interpolated from ECMWF 6hr grids
Radiation pressure model	Tuned 8-panel (Cerri and Ferrage, 2016)	Tuned 8-panel	Thermo-optical coefficient from pre-launch box and wing model, with smoothed Earth shadow model
Tracking data	SLR, DORIS	SLR, DORIS	SLR, DORIS
SLR tropospheric correction model	<del>Mendes and Pavlis (2004)</del> <del>HERS Conventions (2010)</del>	Mendes and Pavlis (2004)	<del>Mendes and Pavlis (2004)</del> <del>HERS Conventions (2010)</del>
DORIS tropospheric correction model	Vienna Mapping Functions 1 (Boehm and Schuh, 2004)	Vienna Mapping Functions 1	GPT2/Vienna Mapping Functions 1
DORIS modelling	DORIS beacon frequency bias modelling	DORIS beacon phase center	DORIS beacon phase center
<del>DORIS system time bias</del>	<del>Estimated once per arc</del>	<del>Estimated once per arc</del>	<del>None</del>
SLR antenna reference	LRA model (note 1 below)	LRA model (note 1 below)	X: 1.2429, Y: -0.0012, Z: 0.8783 in [m]
DORIS antenna reference	pre-launch	pre-launch	pre-launch
SLR / DORIS observation weight	3 cm / 0.05 cm/s	10 cm / 0.2 cm/s	1 cm / 0.03 cm/s

675 Note 1: [https://ilrs.cddis.eosdis.nasa.gov/missions/satellite\\_missions/past\\_missions/topx\\_com.html](https://ilrs.cddis.eosdis.nasa.gov/missions/satellite_missions/past_missions/topx_com.html)

685 **Table 2. Average values of SLR and DORIS RMS fits, radial, cross-track and along-track two-day arc overlaps and the number of the arcs used to compute these values for the reference and fourive test orbits.**

Orbit name	SLR RMS [cm]	DORIS RMS [cm/s]	Radial arc overlap [cm]	Cross-track arc overlap [cm]	Along-track arc overlap [cm]	Number of arcs used for SLR RMS	Number of arcs used for DORIS RMS	Number of arc overlaps used	Comment on the orbit
REF	1.96	0.04778	0.90	6.52	3.65	494	459	433	Reference
SLR	1.59		1.72	7.23	9.54	494	=	425	SLR only
DORIS	=	0.04795	0.88	6.84	2.96	=	459	392	DORIS only
<u>TBias</u>	<u>1.99</u>	<u>0.04785</u>	<u>0.85</u>	<u>6.45</u>	<u>2.78</u>	<u>494</u>	<u>459</u>	<u>433</u>	<u>No DORIS system time bias estimated</u>
ITRF14	1.97	0.04776	0.84	6.45	2.83	494	459	433	ITRF2014
Geoid	1.96	0.04775	0.83	6.43	2.80	494	459	433	EIGEN-6S2

690 **Table 3: Median of time series of global mean height differences and RMS values at crossover points for maximum time lapses of 5 days for all orbit solutions during the period April 1993 – NovSeptember 2004. The highest and lowest values of each quantity are marked bold.**

	REF	GSFC	GRGS	SLR	DORIS	<u>TBias</u>	ITRF14	Geoid
Mean [mm]	-3.1	<b>-1.6</b>	-3.0	-2.7	<b>-4.7</b>	<u>-3.6</u>	-2.8	-2.1
RMS [mm]	49.8	<b>49.5</b>	<b>51.3</b>	51.2	50.7	<u>49.8</u>	49.8	49.7

- 695 **Table 4: Global mean orbit related errors for the total signal, interannual trend variability, and decadal trend. Values were derived from the mean radial orbit differences over the oceans: *REF minus SLR*, *REF minus DORIS*, *REF minus ITRF14*, *REF minus Geoid*, *REF minus GSFC*, *REF minus GRGS* for the period April 1993 – June 2004. The corresponding values for the total sea level are tabulated under SLA.**

	REF-SLR	REF-DORIS	REF-ITRF14	REF-Geoid	REF-GSFC	REF-GRGS	SLA
RMS [mm]	4.2	5.1	1.1	2.0	5.4	7.0	52.5
5-years trend [mm/year]	0.04	0.10	0.02	0.02	0.05	0.10	0.55
Decadal trend [mm/year]	0.01	0.05	0.00	0.00	0.04	0.02	2.89

- 700 **Table 5: Regional orbit related errors for the total and seasonal signal, for interannual trend variability and decadal trend. Values were derived from the radial orbit differences: *REF minus SLR*, *REF minus DORIS*, *REF minus ITRF14*, *REF minus Geoid*, *REF minus GSFC*, *REF minus GRGS* for the periods April 1993 – June 2004.**

	REF-SLR	REF-DORIS	REF-ITRF14	REF-Geoid	REF-GSFC	REF-GRGS
RMS [mm]	7.2	9.3	2.4	3.5	7.4	10.7
Annual amplitude [mm]	1.4	2.1	0.4	3.2	5.4	5.6
5-years trend [mm/year]	0.5	0.6	0.2	0.4	1.2	0.9
Decadal trend [mm/year]	0.2	0.4	0.2	0.4	1.0	0.7

705 Table 6: Global mean differences of interannual trend variability and decadal trend related to the orbit solution. Values were derived from the mean radial orbit differences over the oceans: *Geoid minus GRGS, REF minus DORIS, and REF minus SLRTBias, REF minus DORIS and Geoid minus GRGS* for the period April 1993 – June 2004 from all *trackpasses* and (in brackets) for ascending, descending *trackpasses* separately.

	<u>Geoid-GRGS</u>	<u>REF-DORIS</u>	<u>REF-TBias</u>
<u>Interannual trend [mm/year]</u>	0.05 (0.36, 0.29)	0.10 (0.53, 0.37)	0.01(0.57,0.56)
<u>Decadal trend [mm/year]</u>	-0.01 (0.28, -0.34)	-0.05 (0.19, -0.27)	-0.01(0.08,-0.11)

710

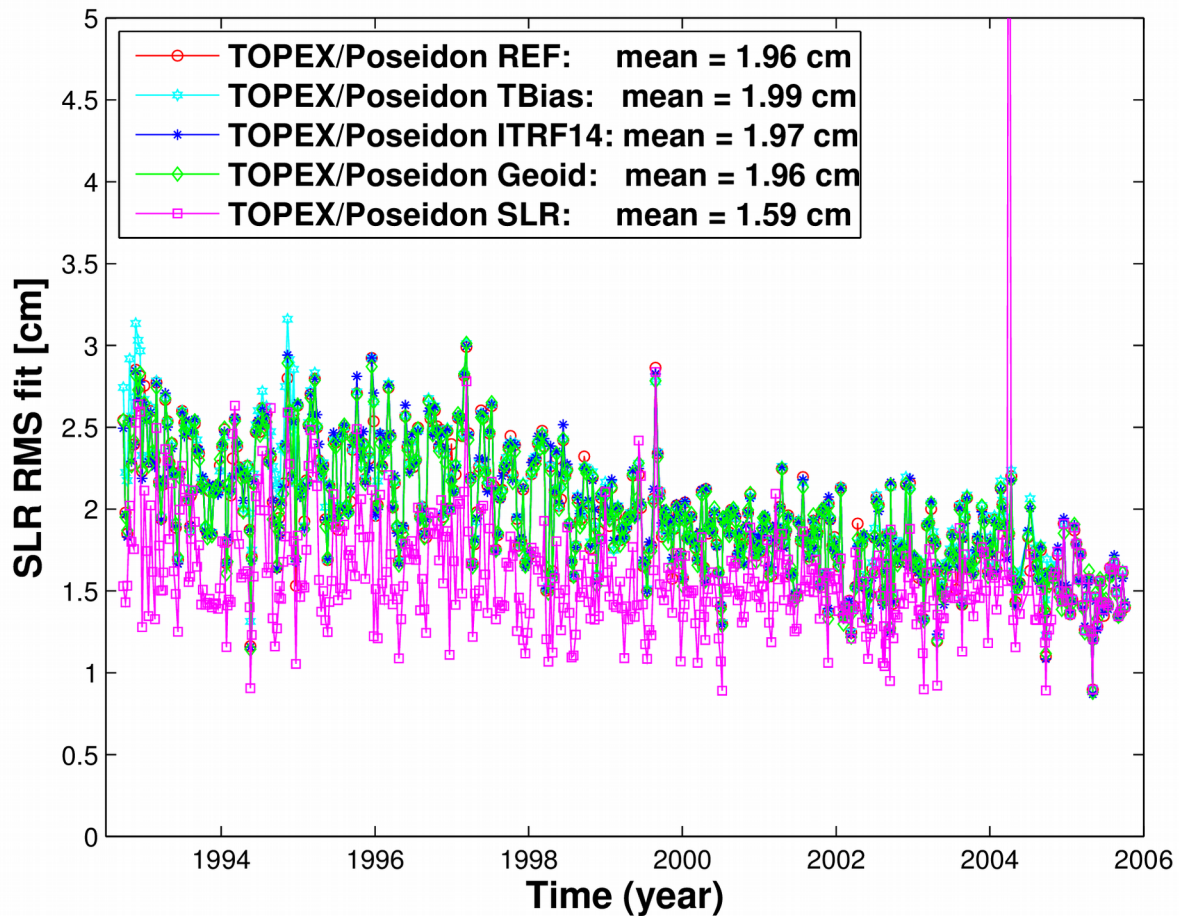


Figure 1: SLR RMS fits of TOPEX/Poseidon REF, SLR, *TBias*, ITRF14, and Geoid orbits.

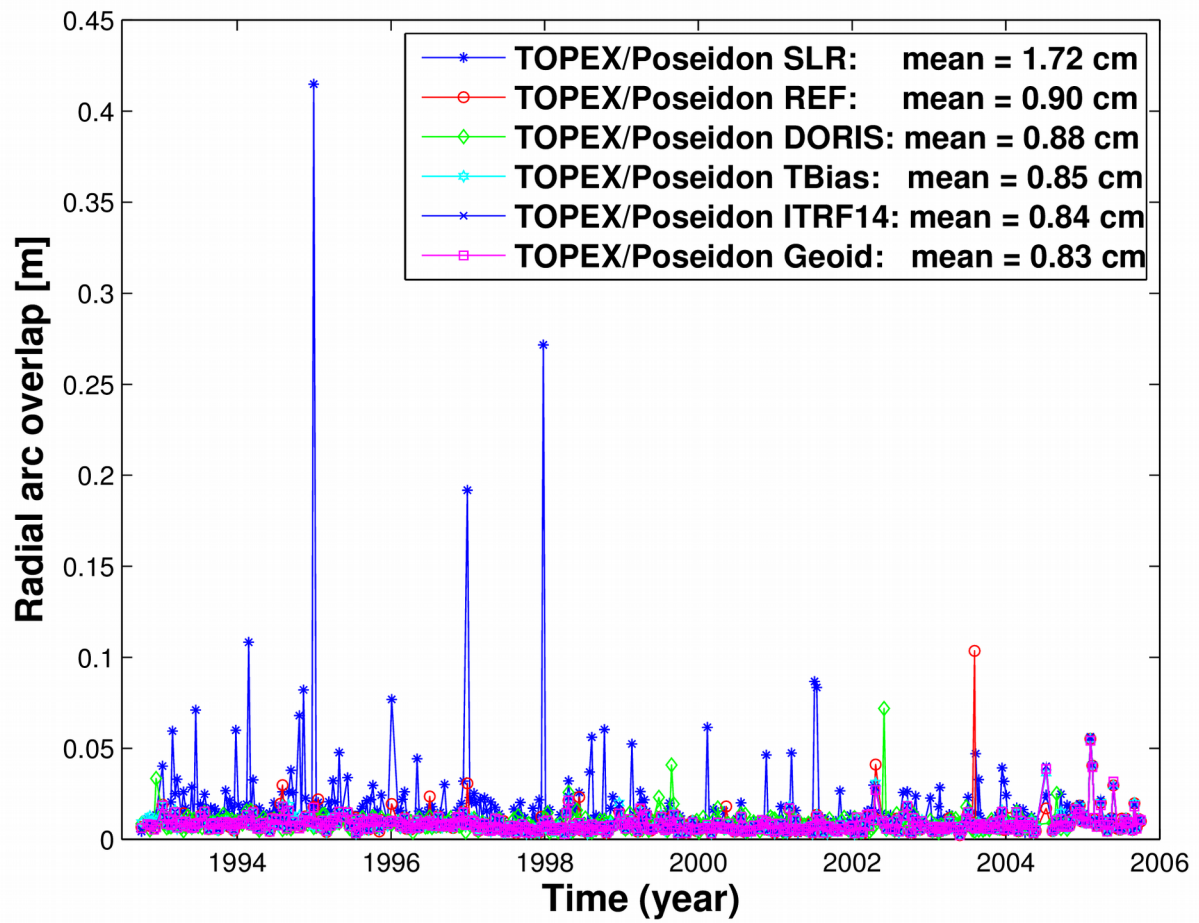
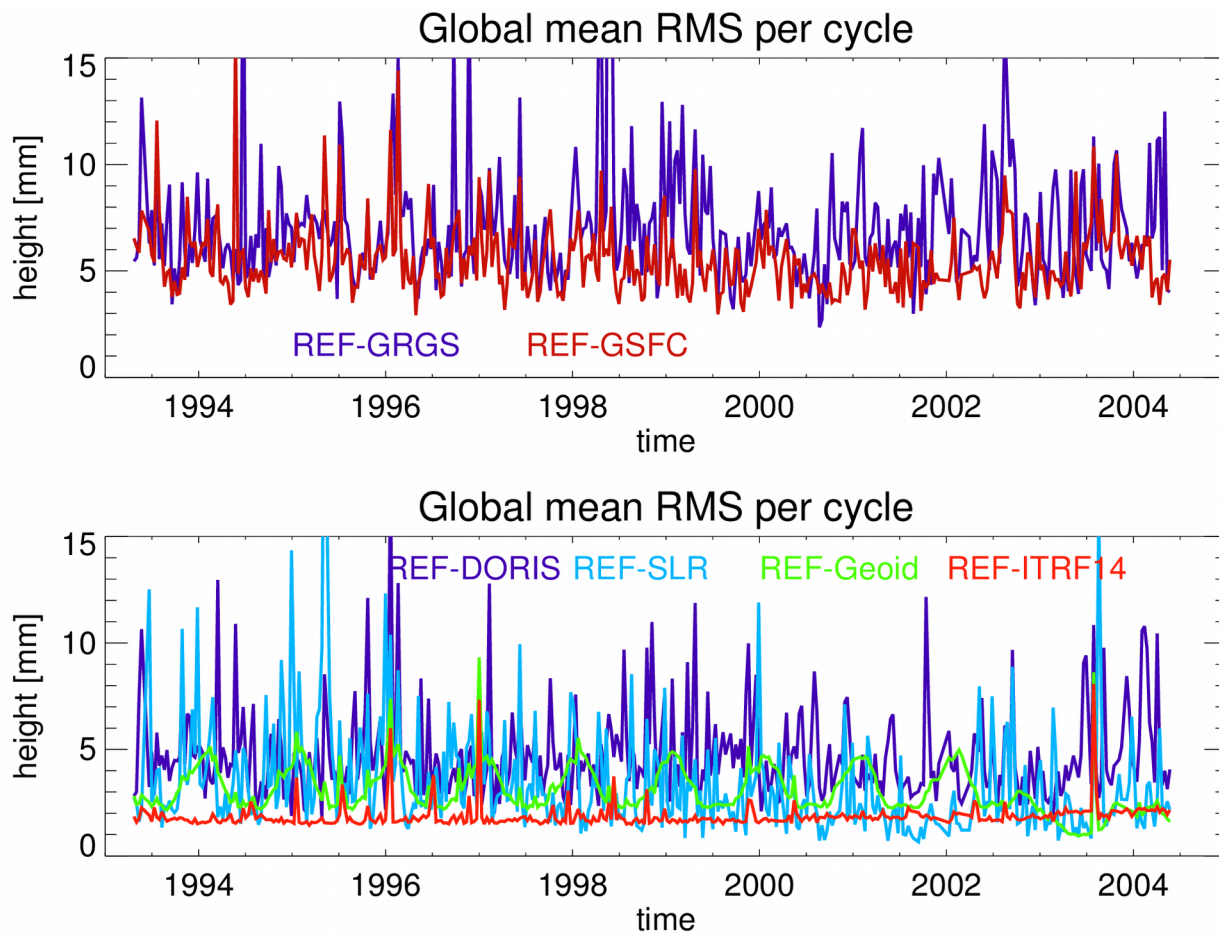
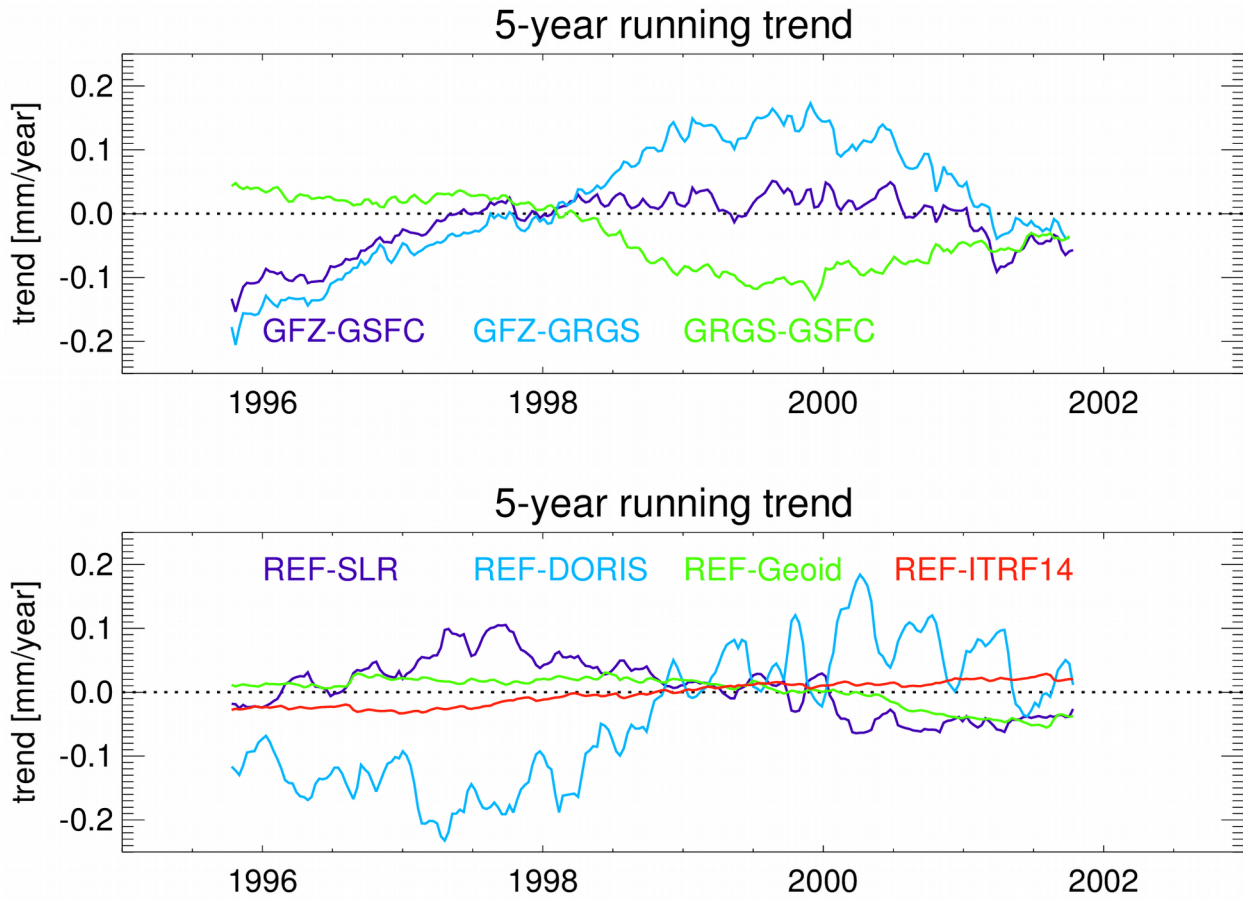


Figure 2. Radial arc overlaps of TOPEX/Poseidon REF, SLR, DORIS, TBias, ITRF14, and Geoid orbits.



735 **Figure 3: Time series of the global mean RMS per cycle over the oceans of gridded radial orbit differences for *REF minus GSFC* (dark blue), and *REF minus GRGS* (red) on the top; for *REF minus DORIS* (dark blue), *REF minus SLR* (light blue), *REF minus Geoid* (green), and *REF minus ITRF14* (red) on the bottom.**



745 | Figure 4: 5-years running trends for the global mean radial orbit differences over the oceans for *REF minus GSFC* (dark blue), *REF minus GRGS* (light blue), and *GRGS minus GSFC* (green) on the top; for *REF minus SLR* (dark blue), *REF minus DORIS* (light blue), *REF minus Geoid* (green), and *REF minus ITRF14* (red) on the bottom. **Trend values are given for the central time of the corresponding running window.**

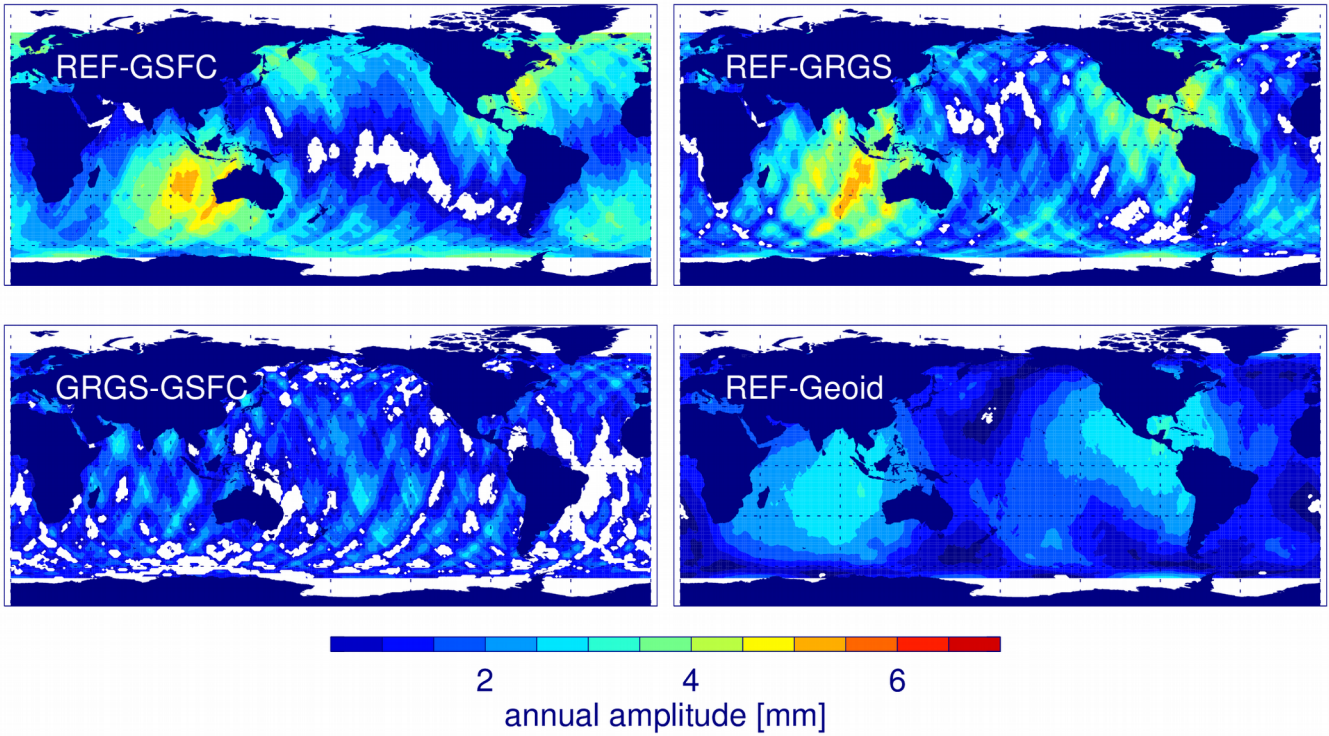
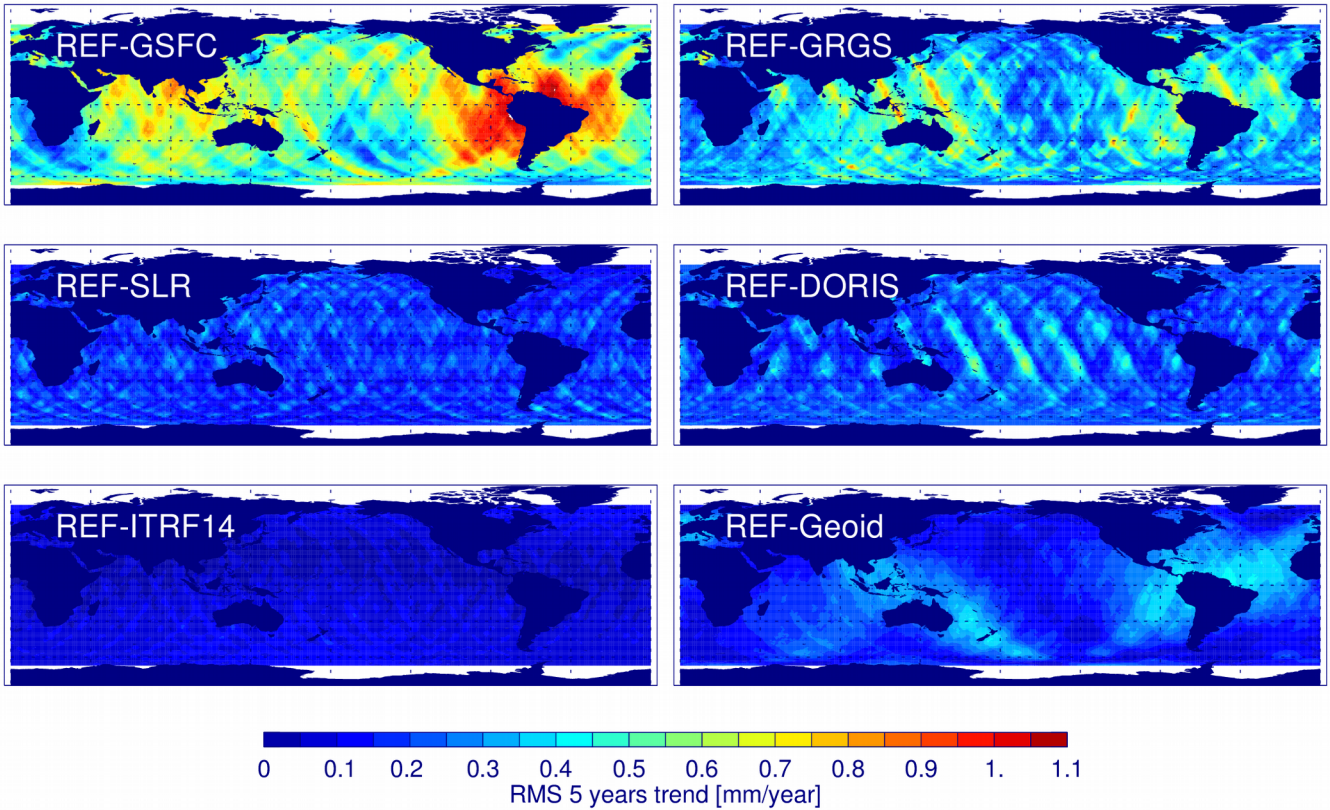


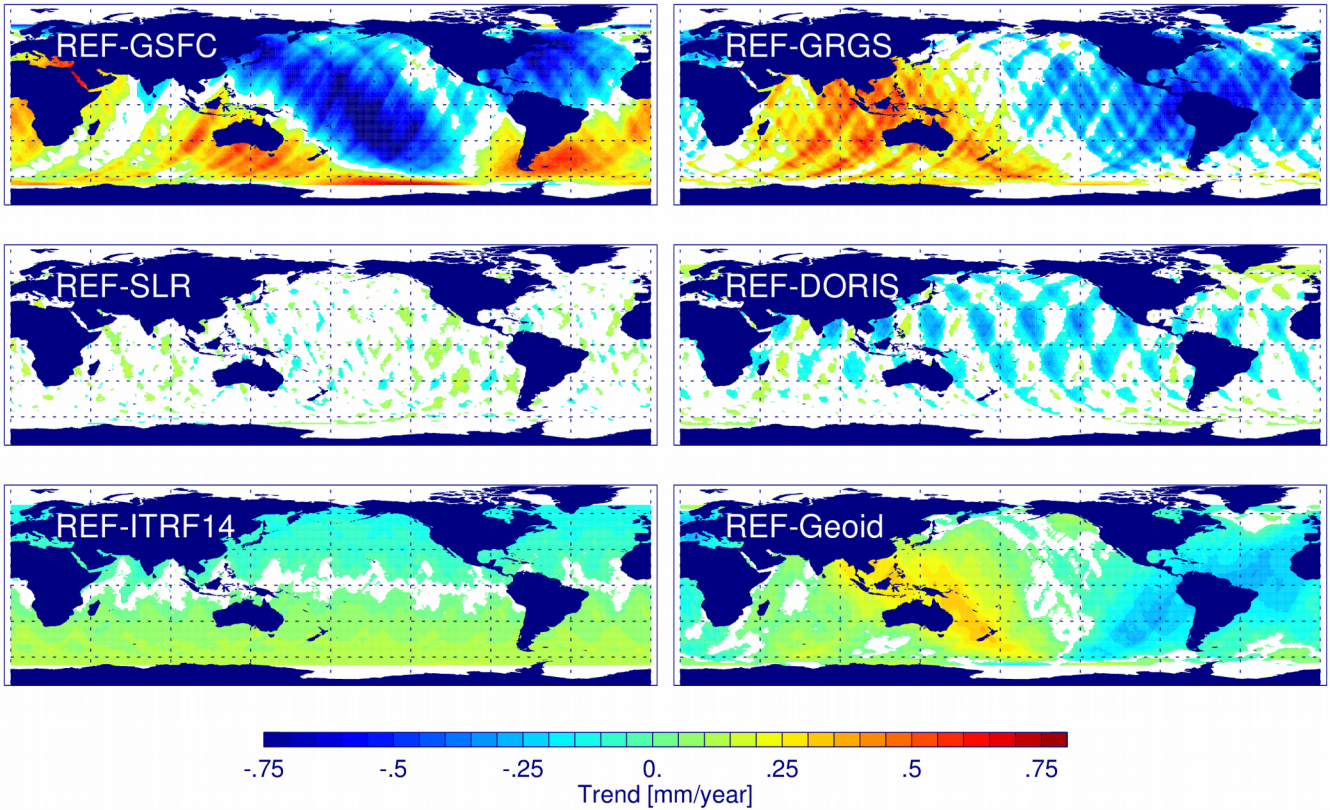
Figure 5: Annual amplitude of the radial orbit differences for *REF minus GSFC*, *REF minus GRGS*, *REFGRGS minus GSFC*, and *REF minus Geoid*. The regions with formal errors larger than the fitted value are masked out (white). The maximum amplitude difference is given in Table 5.



770 | Figure 6: RMS of 5-years running trend differences of the radial orbit components for *REF minus GSFC*, *REF minus GRGS*, *REF*  
*minus SLR*, *REF minus DORIS*, *REF minus ITRF14*, and *REF minus Geoid* for the period April 1993 – June 2004. The global  
775 mean RMS of the differences over the ocean is given in Table 4.

775

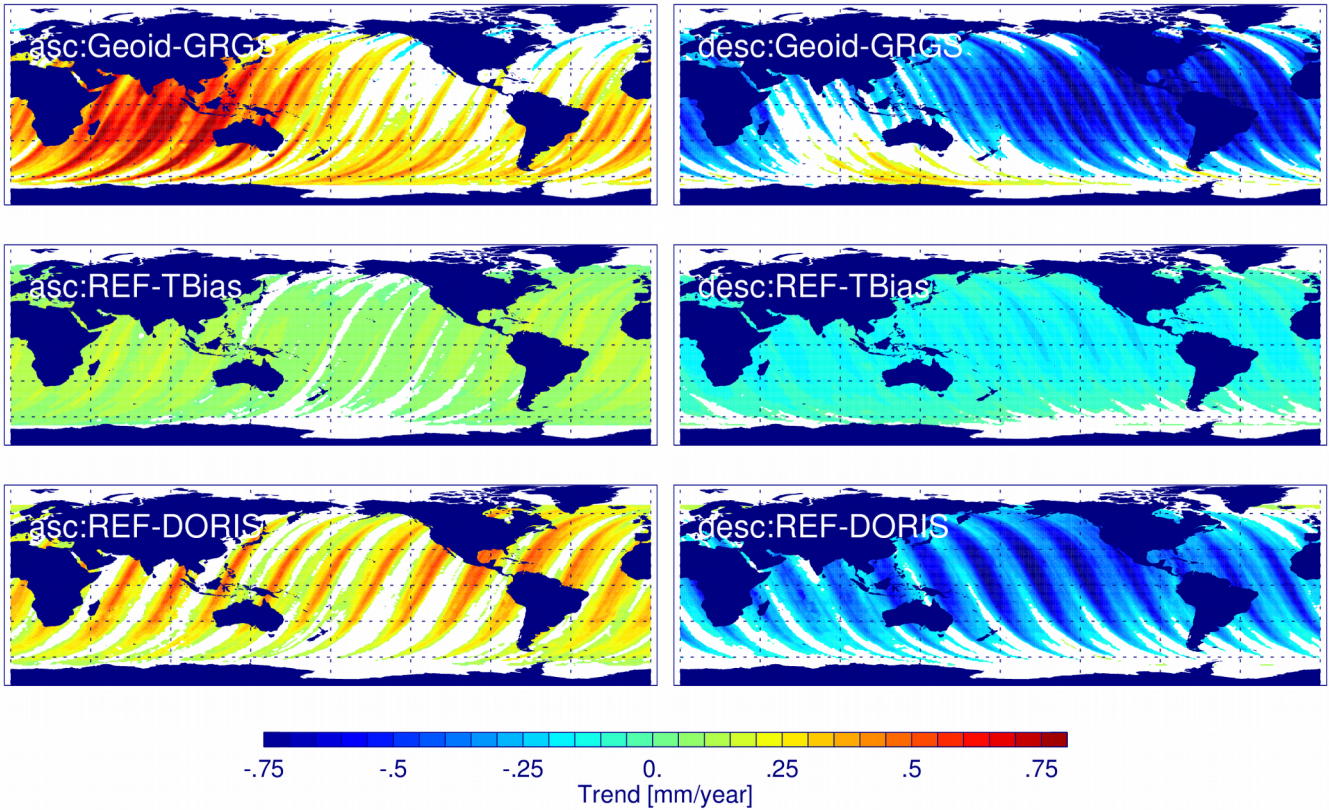
780



785 **Figure 7:** Trend differences of radial orbit components for *REF minus GSFC*, *REF minus GRGS*, *REF minus SLR*, *REF minus DORIS*, *REF minus ITRF14*, and *REF minus Geoid* for the period April 1993–June 2004. Regions with formal errors larger than the fitted value are masked out (white). The global mean trend difference over the ocean is given in Table 4.

790

795



800 | **Figure 89:** Trend differences of radial orbit components for ascending (left) and descending (right) **trackpasses** for *Geoid minus GRGS REF minus TBiasSLR, and REF minus DORIS, and Geoid minus GRGS* for the period April 1993 – June 2004. Regions with formal errors larger than the fitted value are masked out (white). The global mean trend difference over the ocean is given in Table 6.

805

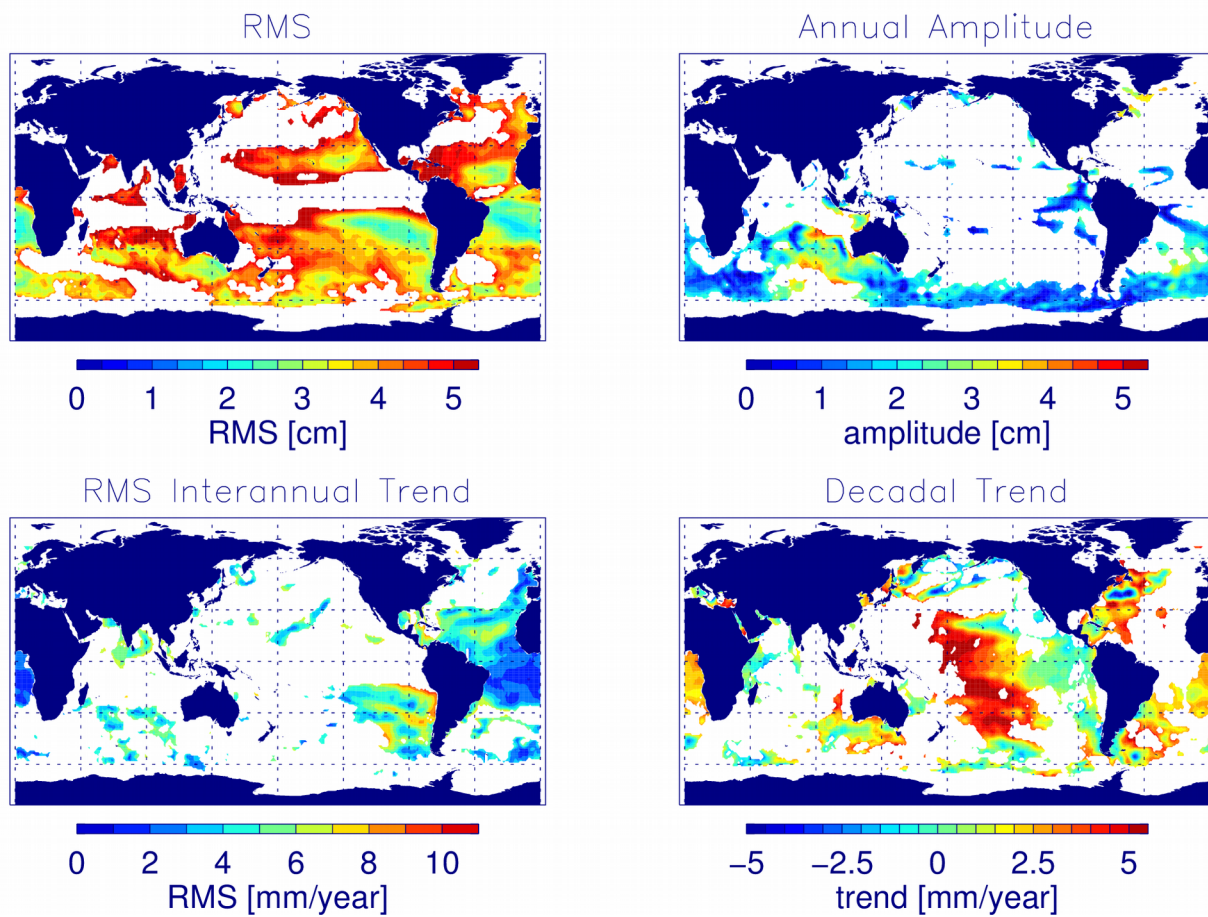


**Figure 9: RMS of sea level, annual amplitude, RMS of interannual (5 years) running trend, and decadal trends from TOPEX altimeter data for the period February 1993– October 2005. Colour coded are sea level values for which the local orbit errors (estimated from *GFZ minus GRGS*) reach more than 10 % of the local sea level values. All other regions are masked out (white).**

810 |

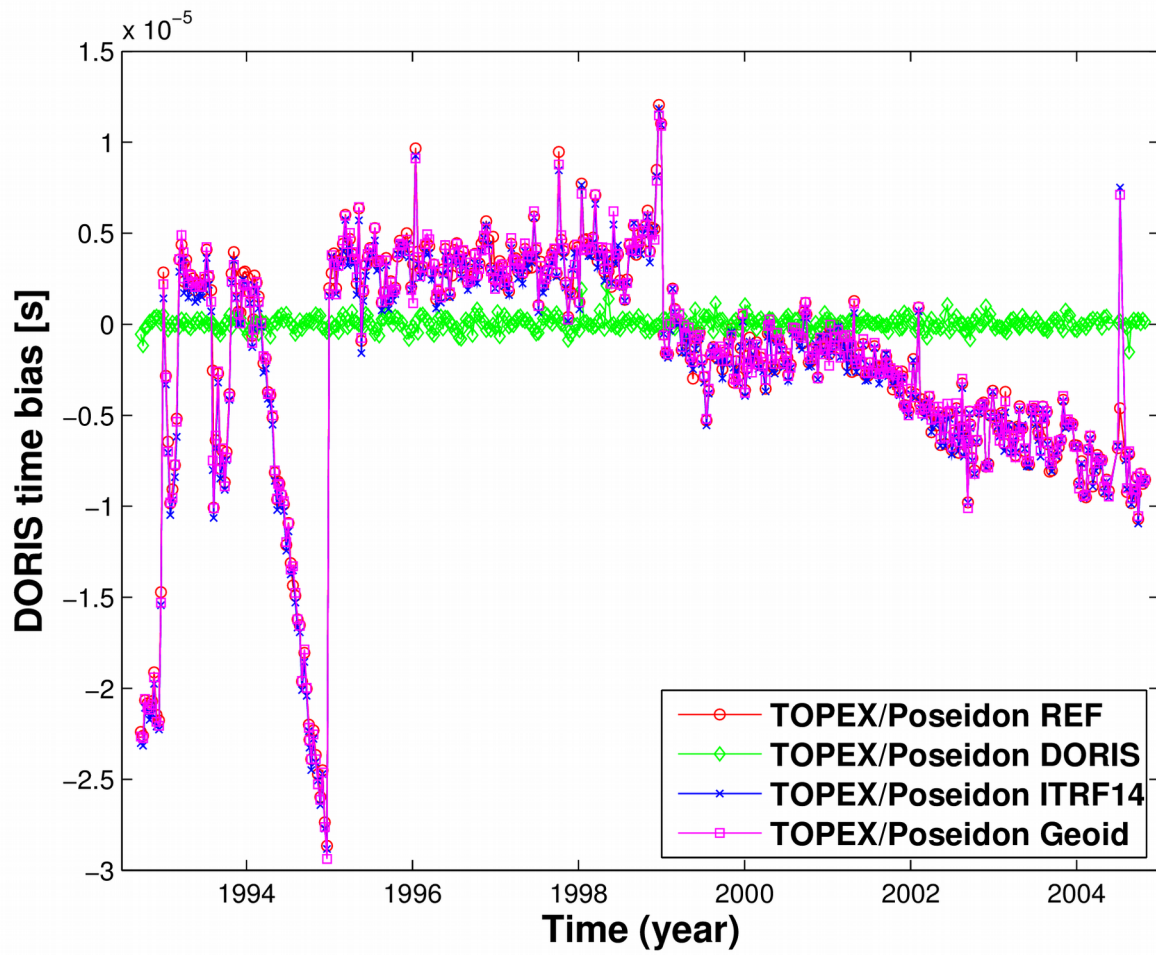
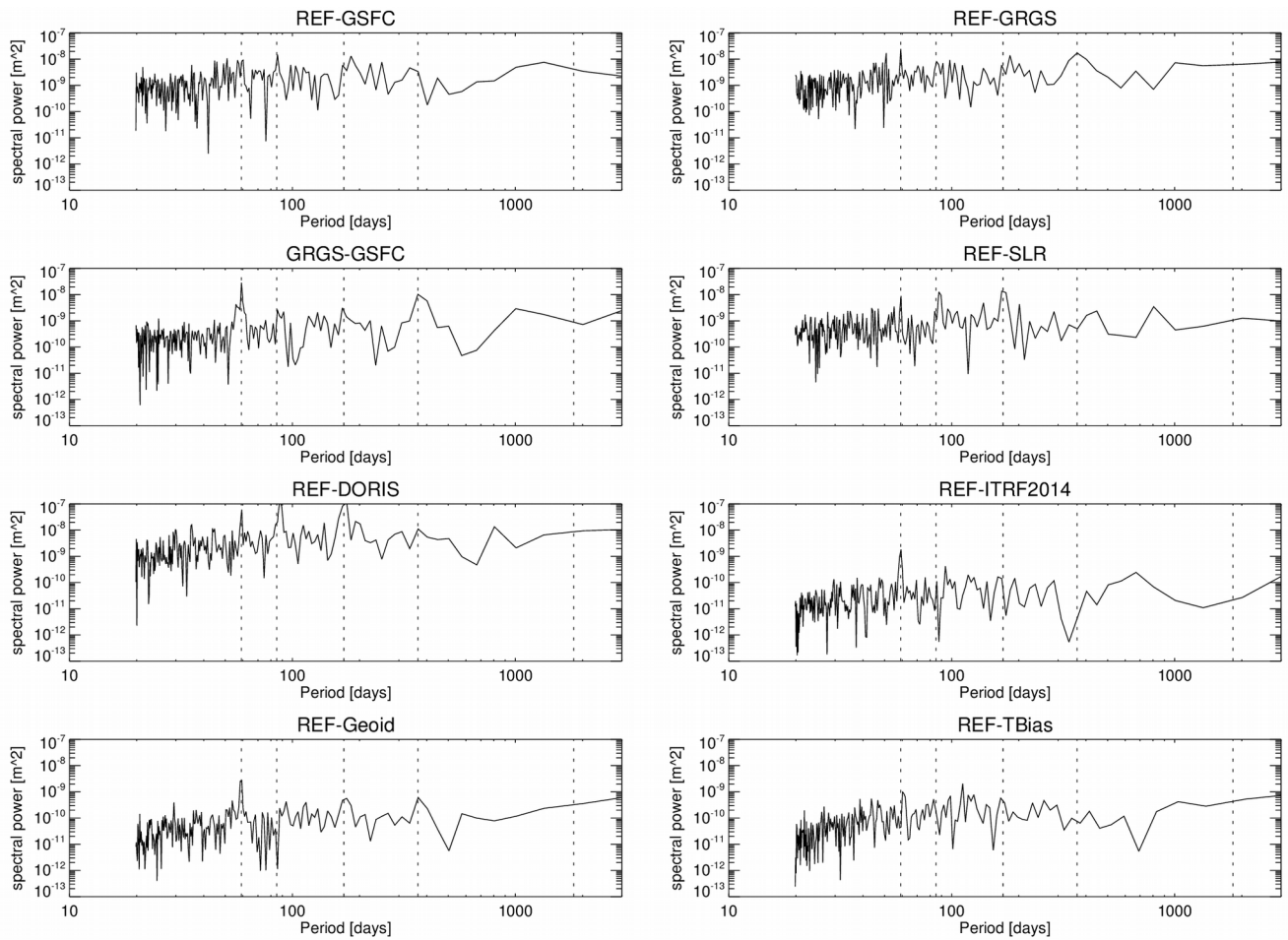
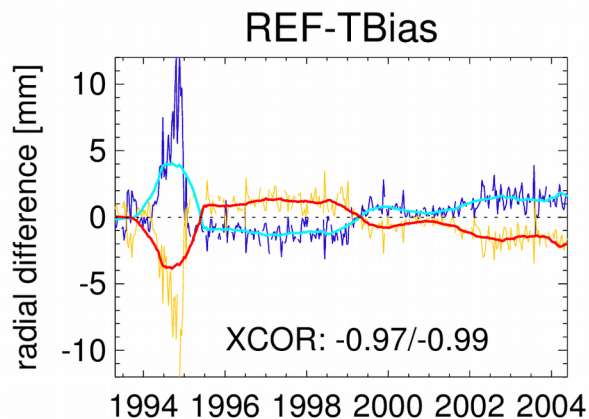
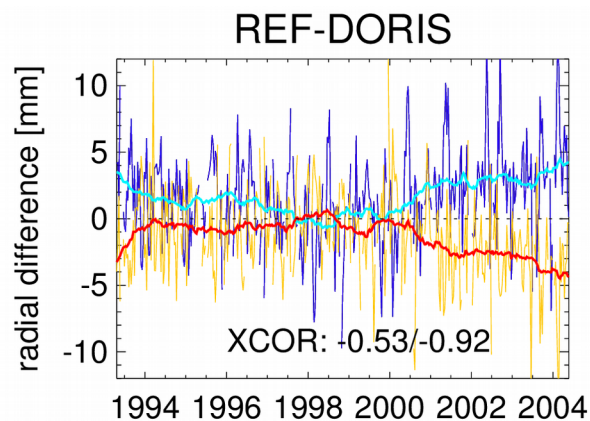
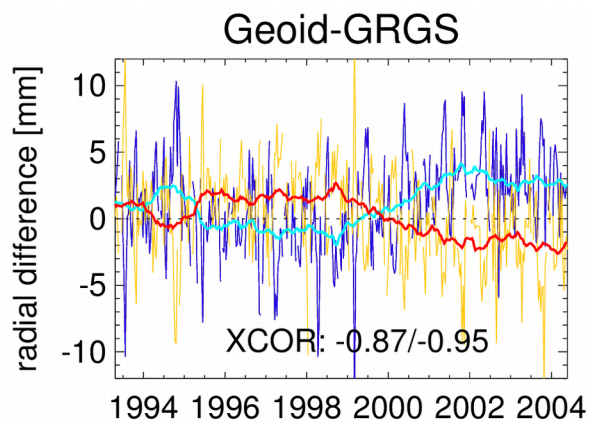


Figure S1: DORIS system time bias of TOPEX/Poseidon REF, DORIS, ITRF14, and Geoid orbits.



815 **Figure S2: Power spectra of the global mean radial orbit differences for *REF minus GSFC*, *REF minus GRGS*, *GRGS minus GSFC*, *REF minus SLR*, *REF minus DORIS*, *REF minus ITRF14*, *REF minus Geoid*, and *REF minus TBias*. Vertical dashed lines mark periods of 59, 85, 170 days, 1 and 5 years.**



820 **Figure S3: Global mean radial orbit differences per cycle for *Geoid minus GRGS*, *REF minus DORIS*, and *REF minus Tbias* separately for ascending (blue, cyan) and descending (yellow, red) tracks and 1-year box-car filtered. The cross-correlation coefficient between the ascending and descending passes for the original and the filtered series is given at the lower part of each graph.**